Structures and Photoactivation of the Charge-Transfer Complexes of Bis(arene)iron(II) Dications with Ferrocene and Arene Donors

R. E. Lehmann and J. K. Kochi*

Contribution from the Department of Chemistry, University of Houston, University Park, Houston, Texas 77204-5641. *Received May 31, 1990. Revised Manuscript Received August 24, 1990*

Abstract: Ferrocene forms a series of unusual charge-transfer crystals with the isoelectronic bis(arene)iron(II) dication, in which X-ray crystallography establishes the alternate (heterosoric) stacking of sandwich structures comprising the donor–acceptor pairs. In acetonitrile, the 1:1 complex [Cp_2Fe, Ar_2Fe^{2+}] shows a broad absorption band centered at $\lambda_{max} \sim 630$ nm. Bis(arene)iron(II) acceptors also form highly colored crystals with various arene donors, in which the charge-transfer absorption ($h\nu_{CT}$) derives from the same heterosoric stacking of donor–acceptor pairs—despite the structurally divergent nature of the arene (planar) and ferrocene (sandwich) donors. These absorptions undergo a predictable red-shift with increasing acceptor strength in the order $(BZ)_2Fe^{2+} > (MES)_2Fe^{2+} > (DUR)_2Fe^{2+} > (HMB)_2Fe^{2+}$, as judged by the reduction potentials $E°_{red}$ of the benzene, mesitylene, durene, and hexamethylbenzene derivatives, respectively. Common to both classes of 1:1 bis(arene)iron(II) complexes [Ar_2Fe^{2+}, D], where D is either a ferrocene or arene donor, is the efficient photoinduced substitution of the arene ligands that occurs in solution when the charge-transfer bands are selectively irradiated with monochromatic light. Time-resolved picosecond spectroscopy identifies such a charge-transfer deligation to occur via the direct photoexcitation of the complex to the ion radical pair, i.e., [Ar_2Fe^{2+}, D] $\xrightarrow{h\nu_{CT}}$ [Ar_2Fe^{+}, $D^{\cdot+}$], followed by the spontaneous loss of arene ligands by the acceptor moiety. Indeed, the substitution lability of the 19-electron intermediate Ar_2Fe^{+} can be independently demonstrated by the application of transient electrochemical methods to the reduction of various bis(arene)iron(II) dications.

Introduction

Ferrocene is a viable electron donor by virtue of its vertical ionization potential of only IP = 6.858 eV in the gas phase and its oxidation potential of $E°_{ox}$ = 0.41 V vs SCE in solution.[1,2] Furthermore, the minimal structural change resulting from the oxidative conversion of ferrocene to ferrocenium ion[3] is symptomatic of the minor reorganization energy requisite for facile electron transfer.[4,5] The electron-rich character of ferrocene is chemically manifested in various reactions. Thus, the rapid substitution of the ferrocene ring by electrophiles is akin to electrophilic aromatic substitution of the most electron-rich arenes, and it typically includes alkylation, acylation, metalation, and sulfonation.[6,7] However, various attempts to effect the corresponding halogenation and nitration of ferrocene with the usual electrophilic reagents such as bromine, nitric acid, etc. merely result in its oxidation to ferrocenium ion.[8,9] Similar to other electron-rich donors, ferrocene also forms neutral charge-transfer (CT) complexes with electron-poor acceptors such as tetracyanoethylene,[9] quinones,[10] polynitroarenes,[11] and various alkyl halides,[12-14] including carbon tetrachloride.[15] Indeed we believe that such weakly bound donor–acceptor pairs are the common intermediates to both substitution and electron transfer of ferrocene—with the electrophile (oxidant) acting as the electron acceptor (A) in the labile precursor complex, i.e.[16]

$$Cp_2Fe + A \rightleftharpoons [Cp_2Fe, A], \text{ etc.} \quad (1)$$

Particularly diagnostic of charge-transfer complexes is the immediate appearance of new spectral bands ($h\nu_{CT}$) when electron donors are mixed with electron acceptors.[17,18] Time-resolved spectroscopic studies have established the charge-transfer bands to derive from the vertical excitation of the donor–acceptor complex to the ion-radical pair, e.g.[19]

$$[Cp_2Fe, A] \xrightarrow{h\nu_{CT}} [Cp_2Fe^{+}, A^{\cdot-}] \quad (2)$$

The mechanistic delineation of such ion-radical pairs is especially relevant to the photoactivation of ferrocene[20] and to the design of organometallic solid-state devices.[21] Thus, the efficient photochemical conversion of ferrocene to ferrocenium chloride in carbon tetrachloride with a quantum yield of near unity is an example[22-25] in which the spontaneous fragmentation within the

(1) Rabalais, J. W.; Werme, L. O.; Bergmark, T.; Karlsson, L.; Hussain, M.; Siegbahn, K. J. *J. Chem. Phys.* **1972**, *57*, 1185.
(2) In acetonitrile; see: Stolzenberg, A. M.; Stershic, M. T. *J. Am. Chem. Soc.* **1988**, *110*, 6391.
(3) Haaland, A. *Acc. Chem. Res.* **1979**, *12*, 415.
(4) Yang, E. S.; Chan, M. S.; Wahl, A. C. *J. Phys. Chem.* **1980**, *84*, 3094.
(5) Sharp, M.; Petersson, M.; Edström, K. *J. Electroanal. Chem.* **1980**, *109*, 271.
(6) (a) Rosenblum, M. E. *Chemistry of the Iron Group Metallocenes*; Wiley: New York, 1965; Part I. (b) Nesmeyanov, A. N.; Perelova, E. G. *Ann. N.Y. Acad. Sci.* **1965**, *125*, 67.
(7) Watts, W. E. In *Comprehensive Organometallic Chemistry*; Wilkinson, G., Stone, F. G. A., Abel, E. W., Eds.; Pergamon: New York, 1982; Vol. 8, pp 1013 ff.
(8) For other examples of electron transfer, see: Watts, W. E. in ref 7.
(9) (a) Rosenblum, M.; Fish, R. W.; Bennett, C. *J. Am. Chem. Soc.* **1964**, *86*, 5166. (b) Collins, R. L.; Pettit, R. *J. Inorg. Nucl. Chem.* **1967**, *29*, 503.
(10) Brandon, R. L.; Osiecki, J. H.; Ottenberg, A. *J. Org. Chem.* **1966**, *31*, 1214.
(11) (a) Hetnarski, B. *Bull. Acad. Pol. Sci., Ser. Sci., Chim.* **1965**, *13*, 515, 523; *Chem. Abstr.* **1966**, *64*, 9093. (b) Hetnarski, B. Ya. *Dokl. Akad. Nauk. SSSR* **1964**, *156*, 604.
(12) Velichko, F. K.; Vasil'eva, T. T.; Kochetkova, V. A.; Vinogradova, L. V.; Balabanova, L. V.; Kartseva, O. S.; Shvekhgeimer, G. A. *Izv. Akad. Nauk SSR, Ser. Khim.* **1967**, 659.
(13) Zver'kov, V. A.; Petrova, A. A.; Vannikov, A. V. *Izv. Akad. Nauk SSR, Ser. Khim.* **1988**, 1399.
(14) Velichko, F. K.; Balabanova, L. V.; Vasil'eva, T. T.; Bondarenko, O. P.; Shvekhgeimer, G. A. *Izv. Akad. Nauk SSR, Ser. Khim.* **1988**, 711.
(15) Brand, J. C. D.; Snedden, W. *Trans. Faraday Soc.* **1957**, *53*, 894.
(16) Kochi, J. K. *Organometallic Mechanisms and Catalysis*; Academic: New York, 1978; Part 3.
(17) See: Foster, R. *Organic Charge-Transfer Complexes*; Academic: New York, 1969.
(18) Andrews, L. J.; Keefer, R. M. *Molecular Complexes in Organic Chemistry*; Holden-Day: San Franciso, CA, 1964.
(19) (a) Hilinski, E. F.; Masnovi, J. M.; Kochi, J. K.; Rentzepis, P. M. *J. Am. Chem. Soc.* **1984**, *106*, 8071. (b) Masnovi, J. M.; Hilinski, E. F.; Rentzepis, P. M.; Kochi, J. K. *J. Am. Chem. Soc.* **1986**, *108*, 1126.
(20) See: (a) Balzani, V.; Carassiti, V. *Photochemistry of Coordination Compounds*; Academic: New York, 1970. (b) Geoffroy, G. L.; Wrighton, M. S. *Organometallic Photochemistry*; Academic: New York, 1979.
(21) Ando, Y.; Nishihara, H.; Aramaki, K. *J. Chem. Soc., Chem. Commun.* **1989**, 1430.
(22) (a) Koerner von Gustorf, E. A.; Koller, H.; Jun, M. J.; Schenck, G. O. *Chem. Eng. Technol.* **1963**, *35*, 591. (b) Koerner von Gustorf, E. A.; Grevels, F. W. *Fortschr. Chem. Forsch.* **1969**, *13*, 366.

0002-7863/91/1513-501$02.50/0

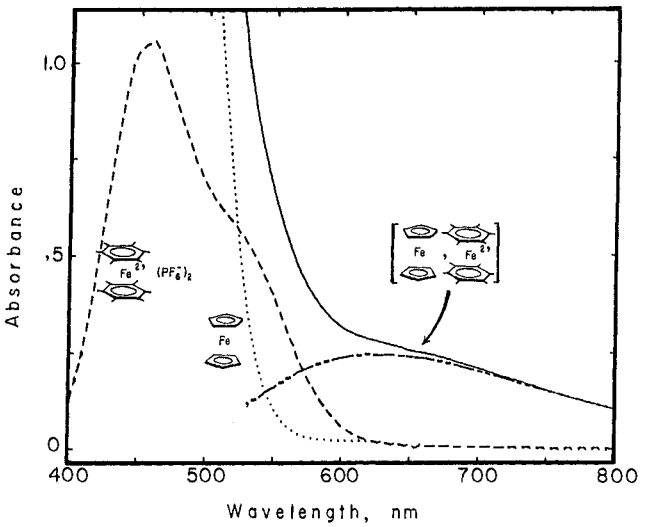

Figure 1. Charge-transfer absorption band (– – –) obtained as a difference spectrum from the visible absorption (—) attendant upon the mixing of 0.09 M ferrocene (···) and 0.03 M $(HMB)_2Fe^{2+}(PF_6^-)_2$ (·–·) in acetonitrile.

first-formed ion pair, i.e., $[Cp_2Fe^{\cdot+}, CCl_4^{\cdot-}] \rightarrow [Cp_2FeCl, CCl_3^{\cdot}]$, etc., effectively competes with its deactivation by back electron transfer.[26] The ion-radical pair pertinent to the configuration mixing of the charge-transfer excited state with the ground state of ferrocene–TCNE complexes has led to bulk ferromagnetic coupling in molecular solids.[27] It is in both of the latter contexts that the preliminary report[28] of the charge-transfer complexes of ferrocene with the isoelectronic bis(arene)iron(II) dication elicits our further interest—particularly arising from the similarity of the (sandwich) structures of these acceptors to that of the ferrocene donor. Accordingly, in this study, we focus first on the isolation and structural characterization of the bis(arene)iron–ferrocene complex by X-ray crystallography and then examine the photochemistry attendant upon the actinic excitation of the charge-transfer band in solution. The CT behavior of ferrocene in comparison with that of the prototypical aromatic donors[29,30] is also an important facet of this study.

Results

I. Charge-Transfer Complexes of Bis(arene)iron(II) and Ferrocene. Spectral Characterization and X-ray Crystallography. When dilute solutions of ferrocene and bis(hexamethylbenzene)iron(II) hexafluorophosphate $(HMB)_2Fe^{2+}(PF_6^-)_2$ in acetonitrile were mixed, the pale yellow-orange mixture instantly took on a dark brown coloration. The spectral change accompanying this dramatic visual transformation is shown in Figure 1 by the obscuration of the visible absorption spectra of ferrocene (dotted curve) and $(HMB)_2Fe^{2+}$ (dashed curve) by an enveloping new absorption at lower energy. Spectra (digital) subtraction revealed the latter as a very broad absorption band with λ_{max} = 626 nm. A similar treatment of ferrocene with the analogous durene dication $(DUR)_2Fe^{2+}$ yielded a corresponding difference spectrum with λ_{max} = 647 nm.[31] The bathochromic shift of 510 cm^{-1} paralleled the relative ease of reduction of the bis(arene)-iron(II) dications as given by their reversible redox potentials (vide infra). The spectral assignment of these broad new absorption bands to intermolecular charge-transfer transitions from the ferrocene donor to the bis(arene)iron(II) acceptors was further confirmed with a variety of aromatic donors, as described in the following section.

The charge-transfer complex spontaneously separated from acetonitrile solution as dark brown, almost black crystals when ferrocene and $(DUR)_2Fe^{2+}$ were employed at higher (0.1 M) concentrations, and single crystals suitable for X-ray crystallography were obtained by the slow diffusive mixing of these solutions.

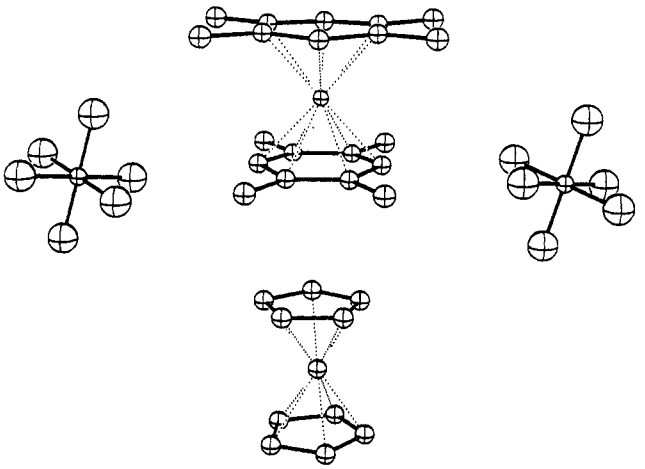

Figure 2. Molecular diagram of the donor–acceptor pair obtained as the 1:1 charge-transfer complex of ferrocene and $(DUR)_2Fe^{2+}(PF_6^-)_2$.

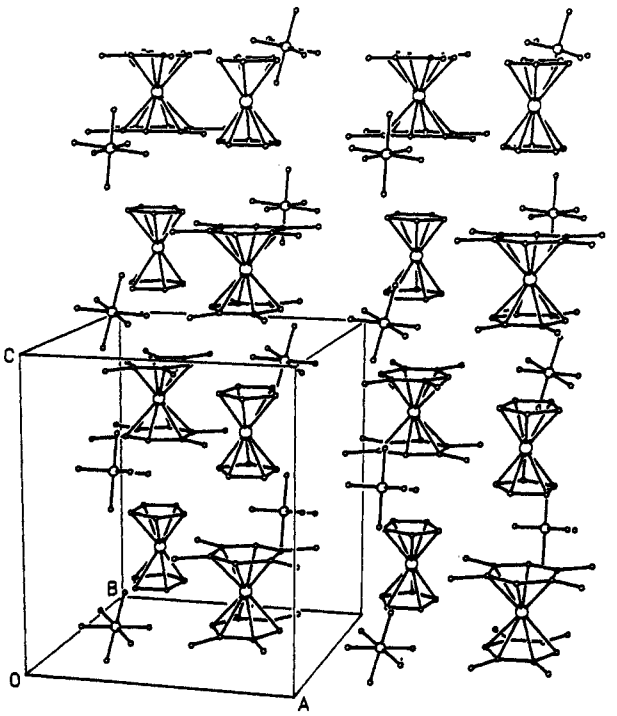

Figure 3. Unit cell of $[Cp_2Fe, (DUR)_2Fe^{2+}(PF_6^-)_2]$ showing the vertical heterosoric stacks of the ferrocene donor and bis(arene)iron(II) acceptor.

(23) (a) Traverso, O.; Scandola, F. *Inorg. Chim. Acta* **1970**, *4*, 493. (b) Traverso, O.; Scandola, F.; Carassiti, V. *Inorg. Chim. Acta* **1972**, *6*, 471.
(24) (a) Akiyama, T.; Hoshi, Y.; Goto, S.; Sugimori, A. *Bull. Chem. Soc. Jpn.* **1973**, *46*, 1851. (b) Akiyama, T.; Sugimori, A.; Hermann, H. *Bull. Chem. Soc. Jpn.* **1973**, *46*, 1855.
(25) Compare also: (a) Bock, C. R.; Wrighton, M. S. *Inorg. Chem.* **1977**, *16*, 1309. (b) Fields, R.; Godwin, G. L.; Haszeldine, R. N. *J. Chem. Soc., Dalton Trans.* **1975**, 1867.
(26) Fox, M. A. *Adv. Photochem.* **1986**, *13*, 237.
(27) See, e.g.: Miller, J. S.; Epstein, A. J.; Reiff, W. M. *Science* **1988**, *240*, 40. Miller, J. S.; O'Hare, D. M.; Chakraborty, A.; Epstein, A. J. *J. Am. Chem. Soc.* **1989**, *111*, 7853.
(28) Braitsch, D. M. *J. Chem. Soc., Chem. Commun.* **1974**, 460.
(29) Howell, J. O.; Goncalves, J. M.; Amatore, C.; Klasinc, L.; Wightman, R. M.; Kochi, J. K. *J. Am. Chem. Soc.* **1984**, *106*, 3968.
(30) See, for example: (a) Wallis, J. M.; Kochi, J. K. *J. Am. Chem. Soc.* **1988**, *110*, 8207. (b) Takahashi, Y.; Sankararaman, S.; Kochi, J. K. *J. Am. Chem. Soc.* **1989**, *111*, 2954.

(31) The instability of bis(benzene)iron(II) in acetonitrile ($\tau_{1/2}$ < 5 h) necessitated the use of the persistent dications $(DUR)_2Fe^{2+}$ and $(HMB)_2Fe^{2+}$ for most of our studies, with an occasional use of $(MES)_2Fe^{2+}$ ($\tau_{1/2} \sim 21$ h).[32]
(32) Compare: Abdul-Rahman, S.; Houlton, A.; Roberts, R. M.; Silver, J. *J. Organomet. Chem.* **1989**, *359*, 331.

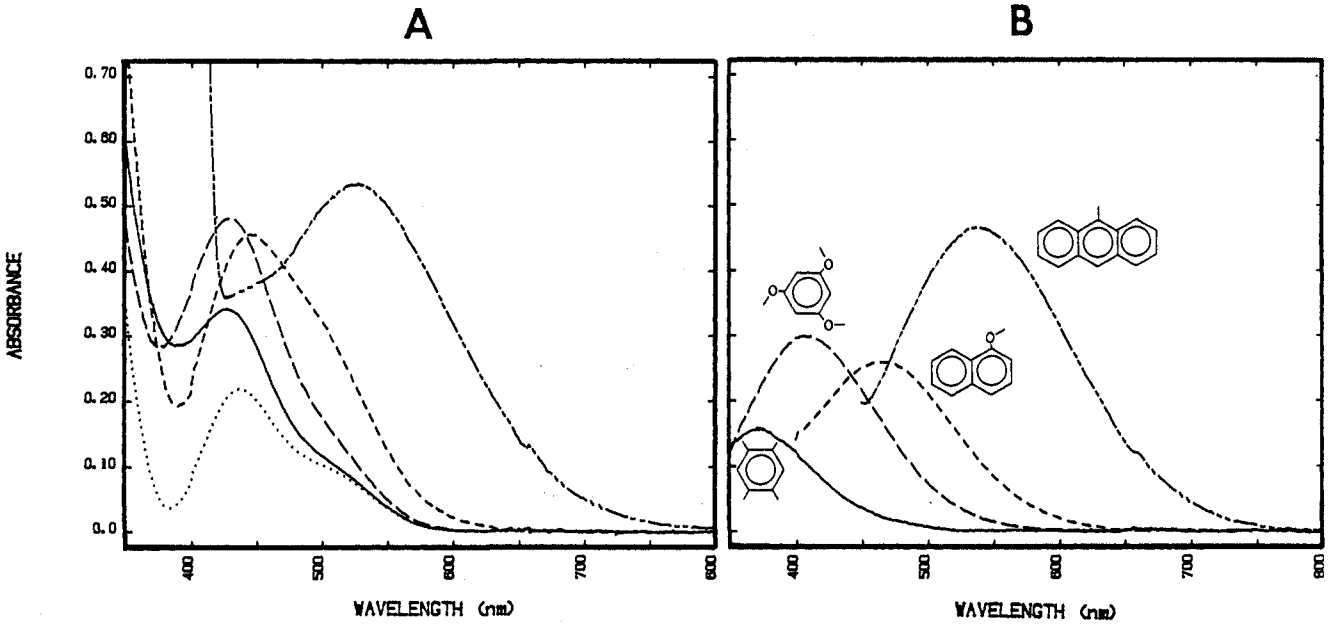

Figure 4. (A) Visible absorption spectrum of 2×10^{-3} $(DUR)_2Fe^{2+}$ alone (···) in acetonitrile and that obtained from added arene donors (0.2 M), as indicated. (B) Charge-transfer spectra of $(DUR)_2Fe^{2+}$ complexes with arene donors generated by digital subtraction of the constituents in (A).

The structure of the charge-transfer complex was solved in the tetragonal space group $P4_2/nmc$ with $a = 11.200$ (3) Å and $c = 13.283$ (5) Å (see full details in the Experimental Section), as a discrete 1:1 mixture of individual ferrocene and bis(durene)-iron(II) hexafluorophosphate units, i.e.

(3)

The ferrocene component maintained its structural integrity within the crystalline complex, and it was observed with an unexceptional disorder of the Cp rings about the rotational axis.[33] By way of contrast, in the $(DUR)_2Fe^{2+}$ acceptor, the coplanar durene rings were rigidly locked in the mutually orthogonal orientation shown in Figure 2. Otherwise the iron–ring (centroid) distance of 1.58 Å in the dication was only slightly less than that (1.66 Å) extant in ferrocene.[34] Importantly, the diagram of the unit cell in Figure 3 shows the stacked alignment of alternating donor–acceptor interactions of Cp_2Fe and $(DUR)_2Fe^{2+}$ units that are separated by the interannular Cp–DUR distance of 3.43 Å. The overall Fe–Fe separation of 6.64 Å within the stack compares with the closest nonbonded Fe–Fe distance of 7.92 Å in the horizontal direction between stacks.

II. Charge-Transfer Complexes of Bis(arene)iron(II) Acceptors and Aromatic Donors. In order to generalize the spectral complexation of the bis(arene)iron(II) acceptor in Figure 1, it was exposed to various arenes whose donor characteristics in charge-transfer complexes were already established.[30] As a test procedure, aliquots of a standard 2×10^{-3} M solution of $(DUR)_2Fe^{2+}(PF_6^-)_2$ in acetonitrile were serially exposed to various arene donors in large (100-fold) excess. The resulting changes in colors ranging from bright yellow for the benzene donors, to red for the naphthalene donors, and finally purple for the anthracene donors corresponded to pronounced alterations of the absorption spectra, as illustrated in Figure 4A for some representative arenes. Digital subtraction of the absorption spectrum of the constituent $(DUR)_2Fe^{2+}$ acceptor yielded the series of broad Gaussian envelopes of the difference spectra in Figure 4B. The monotonic red-shift of the new absorption band with $\lambda_{max} = 368$, 412, 462, and 534 nm coincided with progressively decreasing ionization potentials of IP = 8.05, 7.83, 7.72, and 7.25 eV, for the aromatic donors durene, 1,3,5-trimethoxybenzene, 1-methoxynaphthalene, and 9-methylanthracene, respectively. Such a parallel trend in the absorption band with the donor property of the arenes, as measured by the ionization potential, relates directly to the formation of the charge-transfer complexes, i.e.

$$(DUR)_2Fe^{2+} + Ar \xrightarrow{K} [(DUR)_2Fe^{2+}, Ar] \qquad (4)$$

in accord with the predictions of the Mulliken theory.[35] The charge-transfer absorption bands of other aromatic complexes with $(DUR)_2Fe^{2+}$ are also listed in Table I. The formation constant K in eq 4 could not be reliably evaluated for most aromatic complexes by the spectrophotometric method of Benesi and Hildebrand,[36] owing to inaccuracies inherent in the digital subtraction procedure. However, the clean spectral resolution of the absorption band derived from the strongest donor–acceptor pair allowed the formation constant for the CT complex between 9-methylanthracene and bis(mesitylene)iron(II) to be evaluated as $K = 2.5$ M^{-1} ($\epsilon = 400$ M^{-1} cm^{-1}) in acetonitrile. Since this magnitude of K represented an upper limit for such charge-transfer

Table I. Charge-Transfer Absorption (nm) Spectrum of Bis(arene)iron(II) Complexes with Arene and Ferrocene Donors[a]

arene donor	IP, eV	bis(arene)iron(II) acceptor			
		BZ	MES	DUR	HMB
benzene	9.23	~315	*b*	*b*	
mesitylene	8.42	377	~360	~360	
durene	8.05	385	368	369	*b*
pentamethylbenzene	7.92	411	392	396	380
hexamethylbenzene	7.85	~455[c]	~420[c]	~410[c]	~405[c]
1,3,5-trimethoxybenzene	7.83		412	408	398
1,4-dimethylnaphthalene	7.78			442	
1,5-dimethylnaphthalene	7.74		444	436	428
1-methoxynaphthalene	7.72	486	468	462	451
2,6-dimethoxynaphthalene	7.58	510	503	492	480
9-bromoanthracene	7.47			~485[c]	
9-methylanthracene	7.25	574	550	534	519
diphenylamine	6.94		544	542	526
ferrocene	6.86			647[d]	626[e]

[a] In acetonitrile solution containing 2×10^{-3} M Ar_2Fe^{2+} and 0.2 M donor by spectral (digital) subtraction (see text). [b] λ_{max} not observed. [c] Low solubility, value uncertain. [d] Extrapolated from measured value (665 nm) in $MeNO_2$. [e] 643 nm in $MeNO_2$.

(33) See: Seiler, P.; Dunitz, J. D. *Acta Crystallogr.* **1979**, *B35*, 1068.
(34) Seiler, P.; Dunitz, J. D. *Acta Crystallogr.* **1979**, *B35*, 2020.
(35) Mulliken, R. S. *J. Am. Chem. Soc.* **1952**, *74*, 811.
(36) Benesi, H. A.; Hildebrand, J. H. *J. Am. Chem. Soc.* **1949**, *71*, 2703.

Table II. Wavelength Dependence of the Quantum Yield for Charge-Transfer Deligation[a]

$(DUR)_2Fe^{2+}$, 10^3 M	MeAn, M	λ_{exc}, nm	ϕ	a_{fe}, %	a_{CT}, %	ϕ_{fe}*	ϕ_{CT}*	ϕ_{CT}
2.6	0.18	620	0.18		100		0.18	0.18
9.3	0.15	620	0.18		100		0.18	0.18
9.0	0.08	580	0.25	11	89	0.09	0.16	0.18
4.8	0.15	580	0.23	6	94	0.05	0.18	0.19
5.1	0.20	500	0.34	27	73	0.21	0.13	0.18
8.9	0.07	460	0.47	67	33	0.52	0.05	0.15

[a] In acetonitrile solutions of the $(DUR)_2Fe^{2+}$ complex with 9-methylanthracene (MeAn) at 25 °C. See the Experimental Section for the description of the relative absorbances a_{fe} and a_{CT}, and the (observed) component quantum yields ϕ_{fe}* and ϕ_{CT}*.

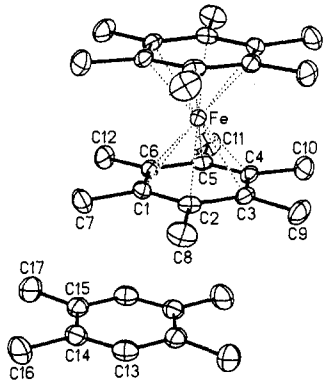

Figure 5. ORTEP diagram of the donor–acceptor pair obtained as the 1:1 charge-transfer complex of durene and $(HMB)_2Fe^{2+}$ (counterion omitted for clarity).

complexes, they are classified[37] in the weak category. The weak complex formulation was also supported by the relatively high concentrations of arene donors generally required to educe the charge-transfer bands in Table I. Nonetheless we were able to successfully grow single crystals of various charge-transfer complexes suitable for X-ray crystallography (see Experimental Section). This class of charge-transfer complexes was typified by the bright orange-red crystals obtained from $(HMB)_2Fe^{2+}$ and durene in the triclinic space group $P\bar{1}$ with a = 9.270 (4) Å, b = 11.040 (5) Å, c = 12.130 (5) Å, α = 71.72 (3)°, β = 67.30 (3)°, and γ = 77.41 (3)°. The ORTEP diagram of the donor–acceptor pair in Figure 5 identifies the durene donor to lie below the hexamethylbenzene ligand (and coplanar with it) at an intermolecular separation of 3.65 Å.[38] The slight displacement of the quasi-C_6 axes could be ascribed to the methyl groups whose closest nonbonded H–H separation of 2.5 Å in Figure 5 would be reduced to only 1.5 Å in the symmetric structure, which is clearly too close for the allowable van der Waals separation of 2.4 Å. Importantly, the diagram of the unit cell in Figure 6 shows the stacked alignment of alternating donor–acceptor interactions of durene and $(HMB)_2Fe^{2+}$ units that are the direct structural counterpart of the ferrocene complex with $(DUR)_2Fe^{2+}$ shown in Figure 3.

III. Photochemistry of the Charge-Transfer Complexes of the Bis(arene)iron(II) Acceptors with Ferrocene and Aromatic Donors. The charge-transfer character of the new absorption bands in Table I was directly examined by the selective electronic excitation of only the complex. For example, an acetonitrile solution of 0.1 M ferrocene and 0.04 M $(HMB)_2Fe^{2+}$ was irradiated with the output from a 450-W xenon lamp passed through a 620-nm interference filter. The use of such a monochromatic irradiation ensured the photoexcitation of only the charge-transfer band of the complex [Cp_2Fe, $(HMB)_2Fe^{2+}$], and not the local bands of either the ferrocene donor or bis(arene)iron(II) acceptor, as established by the comparison of their absorption spectra in Figure 1. The absorption of the 620-nm light was accompanied by the gradual bleaching of the charge-transfer band. Analysis of the photolysate indicated the presence of 2 molar equiv of free hexamethylbenzene identified by its characteristic ^1H NMR spectrum together with 1 equiv of ferrous iron $Fe(MeCN)_6^{2+}$ identified by complexation with 2,2′-bipyridine followed by the spectrophotometric determination of $Fe(bipy)_3^{2+}$ as its characteristic absorption at λ_{max} = 520 nm with ϵ = 8560 M^{-1} cm^{-1}.[40] Since the ferrocene was recovered largely intact, the photochemical conversion of the charge-transfer complex corresponded to the stoichiometry in eq 5.[41] The specific photoexcitation of the charge-transfer band of

$$[Cp_2Fe, (HMB)_2Fe^{2+}] \xrightarrow[MeCN]{h\nu_{CT}} Cp_2Fe + 2HMB + Fe(MeCN)_6^{2+} \quad (5)$$

the ferrocene complex with $(DUR)_2Fe^{2+}$ similarly led to the degradation of the bis(arene)iron(II) acceptor. Since each cationic acceptor was characterized by the loss of the ligand, the photoprocess will be referred to hereafter as *charge-transfer deligation*.[43]

In order to establish the deligation in eq 5 to be a direct consequence of charge-transfer excitation, the ferrocene donor was replaced by a series of arenes with varying donor properties (i.e., ionization potentials). Initially, 9-methylanthracene was chosen as the donor to be used in conjunction with the $(DUR)_2Fe^{2+}$ acceptor, owing to the clean spectral separation of the charge-transfer absorption band from the local absorption of the cationic acceptor. Thus, the use of monochromatic light with λ = 620 ± 5 nm ensured the selective excitation of only the charge-transfer band in Figure 4. Under these conditions, the clean liberation of 2 molar equiv of durene was observed by ^1H and ^{13}C NMR analysis, and the 9-methylanthracene donor (MeAn) was recovered unchanged, together with quantitative yields of $Fe(MeCN)_6^{2+}$ according to the stoichiometry

$$[(DUR)_2Fe^{2+}, MeAn] \xrightarrow[CH_3CN]{h\nu_{CT}} MeAn + 2DUR + Fe(CH_3CN)_6^{2+} \quad (6)$$

The quantum yield for the charge-transfer deligation of $(DUR)_2Fe^{2+}$ by 9-methylanthracene in Table II was measured by Reineckate actinometry and found to be independent of the donor concentration. In order to ascertain the effect of the excitation energy ($h\nu_{CT}$) on the photoefficiency, the incident light was incrementally varied down to 460 nm so that the entire span of the charge-transfer envelope in Figure 4B was covered. Because

(37) Mulliken, R. S.; Person, W. B. *Molecular Complexes*; Wiley: New York, 1969.

(38) It is also interesting to note that the methyl groups in one hexamethylbenzene ligand are eclipsed relative to those on the other ligand, contrary to the staggered (rotational) conformation in the analogous decamethylferrocene.[39]

(39) (a) Freyberg, D. P.; Robbins, J. L.; Raymond, K. N.; Smart, J. C. *J. Am. Chem. Soc.* **1979**, *101*, 892. (b) Struchkov, Yu. T.; Andrianov, V. G.; Sal'nikov, T. N.; Lyatifov, I. R.; Matevikova, R. B. *J. Organomet. Chem.* **1978**, *145*, 213. (c) Almennigen, A.; Haaland, A.; Samdal, S.; Brunvoll, J.; Robbins, J. L.; Smart, J. C. *J. Organomet. Chem.* **1979**, *173*, 293.

(40) Compare the values in water: λ_{max} = 522 nm, ϵ = 8700 M^{-1} cm^{-1}. Busch, D. H.; Bailar, J. C., Jr. *J. Am. Chem. Soc.* **1956**, *78*, 1137.

(41) The presence of ferrocenium ion in small amounts was especially noted with $(DUR)_2Fe^{2+}$, and it was indicated by the residual absorbance at 620 nm.[42]

(42) For Cp_2Fe^+ in aqueous perchloric acid, see: Wilkinson, G.; Rosenblum, M.; Whiting, M. C.; Woodward, R. B. *J. Am. Chem. Soc.* **1952**, *74*, 2125.

(43) The quantum yields for charge-transfer deligation could not be accurately measured owing to a broad residual absorbance between 600 and 800 nm (see Experimental Section).

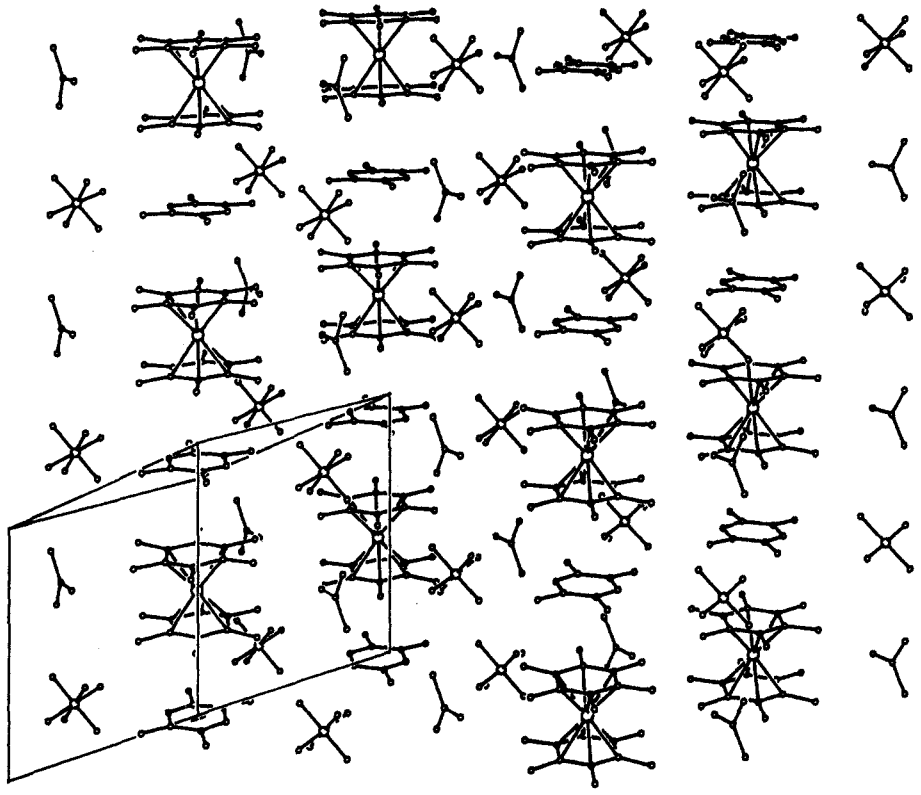

Figure 6. Unit cell of the charge-transfer complex [durene, $(HMB)_2Fe^{2+}(PF_6^-)$] showing the alternating donor–acceptor pairs with the same structural relationship as that in the ferrocene complex in Figure 3.

Table III. Photoefficiency of the Charge-Transfer Deligation of Bis(arene)iron(II) Complexes with Arene Donors[a]

arene	λ_{CT},[b] nm	IP, eV	ϕ_{CT}[b]
mesitylene	~360	8.42	0.56 (2)
durene	369	8.05	0.52 (3)
pentamethylbenzene	393	7.92	0.54 (3)
1,3,5-trimethoxybenzene	408	7.83	0.44 (3)
1,5-dimethylnaphthalene	436	7.74	0.45 (2)
1-methoxynaphthalene	462	7.72	0.36 (2)
1-methylanthracene	534	7.25	0.18 (1)[e]
	550[c]	7.25	0.14 (1)[f]
	519[d]	7.25	0.0080 (10)[f]
diphenylamine	542	6.94	0.059 (5)[f]
	544[c]	6.94	0.054 (5)[f]
	526[d]	6.94	0.0028 (10)[f]

[a] With (2–7) × 10^{-3} M Ar_2Fe^{2+} and 0.2–1.0 M arene in acetonitrile at λ_{exc} = 440 nm. [b] $(DUR)_2Fe^{2+}$, unless indicated otherwise. Significance of the last digit(s) in parentheses. [c] $(MES)_2Fe^{2+}$. [d] $(HMB)_2Fe^{2+}$. [e] λ_{exc} = 500 nm. [f] λ_{exc} = 620 nm.

of spectral overlap shown in Figure 4A, the quantum yields measured at the higher excitation energies required a correction for the photolysis of $(DUR)_2Fe^{2+}$, as described in the Experimental Section. Nonetheless, the results in the last column of Table II were sufficient to establish the photoefficiency (ϕ_{CT}) of the deligation to be largely independent of the CT excitation energy. However the photoefficiency of the charge-transfer deligation of bis(arene)iron(II) acceptors was strongly dependent on the aromatic donor strength, as indicated by the substantial variation in the quantum yields listed in Table III. Indeed the trend in the values of ϕ_{CT} for different donors was quite remarkable—in that the weaker donors induced the markedly higher quantum efficiencies.

IV. Time-Resolved Spectroscopy of Reactive Intermediates in Charge-Transfer Deligation of Bis(arene)iron Acceptors. The reactive intermediates leading to the charge-transfer deligation of the bis(arene)iron(II) acceptors in eqs 5 and 6 were examined by time-resolved picosecond spectroscopy immediately following the application of an 18-ps laser pulse. By the appropriate choice of bis(arene)iron(II) concentration, the 532-nm pulse (obtained by the frequency doubling of the output of the Nd^{3+}:YAG laser) was optimally utilized to excite the charge-transfer band of the Cp_2Fe–$(HMB)_2Fe^{2+}$ complex for the deligation according to eq 5. The time-resolved spectrum presented in Figure 7 showed a strong resemblance to the absorption spectrum previously obtained from an authentic crystal of the monocationic $(HMB)_2Fe^+PF_6^-$ with λ_{max} = 580 nm (ϵ = 604 M^{-1} cm^{-1})[44] as well as the spectrum of ferrocenium ion with λ_{max} = 619 nm (ϵ = 360 M^{-1} cm^{-1}).[42] A similar spectral transient (albeit weaker) was observed when the $(DUR)_2Fe^{2+}$ complex with ferrocene was subjected to the 532-nm laser flash. Such one-electron redox changes of the donor–acceptor pair accorded with the Mulliken formulation of the charge-transfer excitation of weak complexes.[45] Scrutiny of the absorption spectra

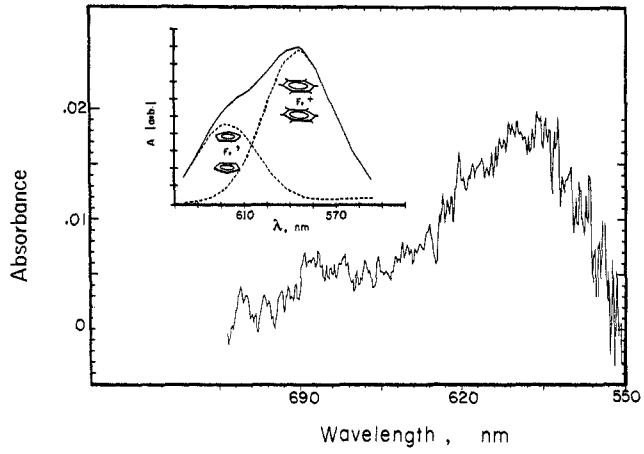

Figure 7. Transient absorption spectrum taken at 40 ps following the application of the 532-nm laser pulse to a solution of 0.1 M ferrocene and 0.03 M $(HMB)_2Fe^{2+}$ in acetonitrile. The inset shows the Gaussian deconvolution based on the spectra of $(HMB)_2Fe^+$ (λ_{max} = 580 nm, ϵ = 604 M^{-1} cm^{-1})[42] and Cp_2Fe^+ (λ_{max} = 620 nm, ϵ = 360 M^{-1} cm^{-1}).[44]

(44) In acetone; see: Fischer, E. O.; Röhrscheid, F. *Z. Naturforsch.* **1962**, *17b*, 483.

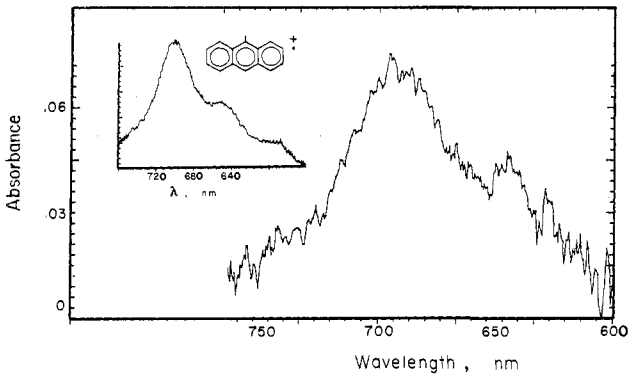

Figure 8. Transient spectrum (33 ps) obtained from the charge-transfer excitation at 532 nm of a solution of 0.2 M 9-methylanthracene and 0.0034 M $(HMB)_2Fe^2$. The inset shows the time-resolved spectrum of 9-methylanthracene cation radical[50] for comparison.

in Figure 7, however, indicated that the CT excitation of the complex at 532 nm was somewhat complicated by the partial spectral overlap at 532 nm of the local band of the acceptor moiety.[46] This ambiguity could be minimized in the photoexcitation of the bis(arene)iron(II) complexes with 9-methylanthracene, in which the CT absorptions were resolved from the absorption bands of the acceptor (See Figure 4). Particularly well suited for the 532-nm excitation were the charge-transfer complexes from $(HMB)_2Fe^{2+}$ and $(DUR)_2Fe^{2+}$ with 9-methylanthracene, especially when the donor was employed in large excess.[47] For example, Figure 8 shows the transient absorption spectrum obtained at 33 ps following the CT excitation of the acetonitrile solution of 0.003 M $(HMB)_2Fe^{2+}$ and 0.2 M 9-methylanthracene. The identical spectral transient was obtained when an otherwise equivalent solution prepared from $(DUR)_2Fe^{2+}$ was irradiated with the 532-nm laser pulse. In both cases, the transient absorption corresponded to the authentic spectrum of the 9-methylanthracene cation radical ($MeAn^{\cdot+}$) that was unambiguously generated by the γ-radiolysis[48] or anodic[49] or photoinduced[50] oxidation of 9-methylanthracene; and it is shown for comparison in the inset to Figure 8.[51]

V. Electrochemical Reduction of the Bis(arene)iron(II) Acceptor. The bis(arene)iron(II) dications were evaluated as electron acceptors at a platinum electrode in acetonitrile solutions containing 0.1 M tetra-*n*-butylammonium hexafluorophosphate (TBAH) as the supporting electrolyte. Cyclic voltammetry and double-step chronoamperometry were particularly useful in identifying the transient phenomena associated with the reduction. Thus, the initial negative-scan cyclic voltammetry of the bis(arene)iron(II) complexes (containing mesitylene, durene, or hexamethylbenzene ligands) all exhibited a pair of one-electron cathodic waves P_1 and P_2 for the reduction of these dications to the 19-electron monocation bis(arene)iron(I) and the 20-electron neutral complex bis(arene)iron(0),[53] respectively, i.e.

$$Ar_2Fe^{2+} \overset{P_1}{\rightleftharpoons} Ar_2Fe^{+} \overset{P_2}{\rightleftharpoons} Ar_2Fe^{0} \qquad (7)$$

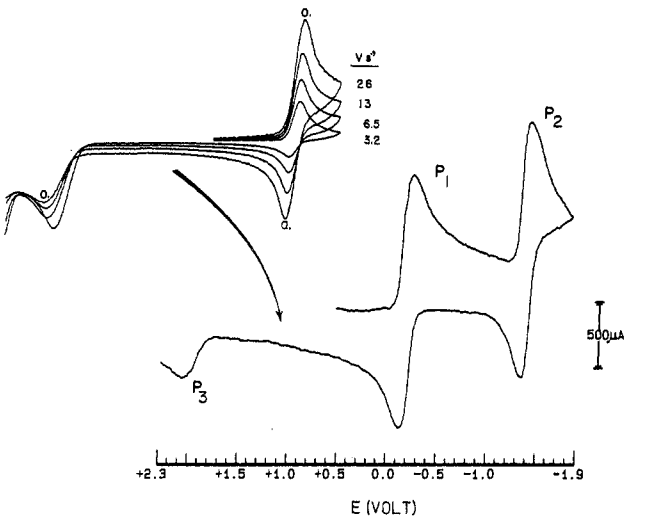

Figure 9. Initial negative-scan cyclic voltammogram of 4.2×10^{-3} M $(DUR)_2Fe^{2+}$ in acetonitrile containing 0.1 M TBAH at $v = 200$ V s^{-1}. The inset shows the scan rate dependence of the current ratio i_p^a/i_p^c of the first wave (P_1) and of the peak current of the anodic wave P_3.

Table IV. Cathodic Reduction of Bis(arene)iron(II) Acceptors in Acetonitrile[a]

$(Ar)_2Fe^{2+}$ arene	v_{min},[b] V s^{-1}	E°_1, V	E°_2, V	E_p,[c] V
mesitylene	500	−0.06	−1.27	2.25
durene	100	−0.16	−1.38	1.98
hexamethylbenzene	5	−0.26	−1.46	1.67

[a] In solutions containing 5×10^{-3} M $Ar_2Fe^{2+}(PF_6^-)_2$ and 0.1 M TBAH at 25 °C. [b] See text. [c] Irreversible anodic wave on the return at slower scan rates. All potentials given in volts vs SCE.

Figure 9 illustrates the typical cyclic voltammogram for the reduction of $(DUR)_2Fe^{2+}$, with the 2+/+ and +/0 waves at $E^\circ_{red} = -0.16$ and −1.38 V vs SCE, respectively. Both waves of $(DUR)_2Fe^{2+}$ were chemically reversibly only at the relatively high scan rates of $v_{min} = 100$ V s^{-1}, as indicated by the ratios of the anodic/cathodic peak currents of $i_p^a/i_p^c = 1.0$. The current ratio gradually decreased at successively slower CV scan rates, and finally the value of i_p^a/i_p^c for the first reduction fell to only 0.1 at $v = 1.0$ V s^{-1}. Coincident with such a diminishing degree of CV reversibility was the appearance on the return positive scan of a new anodic wave P_3 with increasing peak current, as shown in the inset to Figure 9. This anodic peak was readily assigned to the oxidation of durene, by comparison with that of an authentic sample of the free (DUR) ligand. The new anodic wave P_3 was observed only after the initial negative voltammetric scan was swept out to P_1—the initial positive-scan cyclic voltammogram of $(DUR)_2Fe^{2+}$ showing no anodic peak P_3. (Furthermore the anodic current of P_3 was markedly diminished at rapid return scans.) These observations, coupled with the scan rate variation of i_p^a/i_p^c (vide supra) and further double-step chronoamperometric studies,[54] established the degradative cathodic process to be associated with the deligation of the transient monocation,[55] e.g.

$$(DUR)_2Fe^{+} \xrightarrow[(MeCN)]{\text{fast}} 2DUR + Fe^{+}, \text{ etc.} \qquad (8)$$

The related acceptors $(HMB)_2Fe^{2+}$ and $(MES)_2Fe^{2+}$ qualitatively showed the same transient electrochemical behavior, and in each case, the free ligands (HMB and DUR) were observed

(45) For the time-resolved spectroscopic studies of charge-transfer excitation, see: Hilinski, E. F.; et al. in ref 19.

(46) The absorption spectra of $(HMB)_2Fe^{2+}$ and $(MES)_2Fe^{2+}$ are essentially as that of $(DUR)_2Fe^{2+}$, shown in Figure 4A. The spectrum of $(BZ)_2Fe^{2+}$ is also similar, but blue-shifted.

(47) For example, in acetonitrile solutions of 0.2 M 9-methylanthracene and 3.4×10^{-3} M $(HMB)_2Fe^{2+}$ ~80% of the light at 532 nm is absorbed by the complex.

(48) See: Shida, T. *Electronic Absorption Spectra of Radical Ions*; Elsevier: New York, 1988.

(49) Compare: Masnovi et al. in ref 19.

(50) Sankararaman, S., unpublished results by the method of: Miyasaka, H.; Ojima, S.; Mataga, N. *J. Phys. Chem.* **1989**, *93*, 3380. See also: Mataga, N. *Pure Appl. Chem.* **1984**, *56*, 1255.

(51) Note the significantly higher extinction coefficient of $\epsilon = 7700$ M^{-1} cm^{-1} for the anthracene cation radical[52] overshadowed the weaker absorbance of $(HMB)_2Fe^{+}$ at $\lambda = 580$ nm ($\epsilon = 604$ M^{-1} cm^{-1}) in Figure 8.

(52) Torikai, A.; Kato, R. *J. Polym. Sci., Polym. Chem. Ed.* **1978**, *16*, 1487. See also: Reference 45.

(53) For the isolation of $(HMB)_2Fe^{+}$ and $(HMB)_2Fe$, see: Fischer, E. O.; Röhrscheid, F. in ref 44. See also: Braitsch, D. M.; Kumarappan, R. *J. Organomet. Chem.* **1975**, *84*, C37.

(54) Karpinski, Z.; Kochi, J. K., to be published.

(55) For previous observations on the transient character of bis(arene)-iron(I) monocations, see: (a) Michaud, P.; Mariot, J.-P.; Varret, F.; Astruc, D. *J. Chem. Soc., Chem. Commun.* **1982**, 1383. (b) Anderson, S. E.; Drago, R. S. *J. Am. Chem. Soc.* **1970**, *92*, 4244. Dissociative or associative mechanisms for deligation are unclear owing to the possibility of ring slippage.

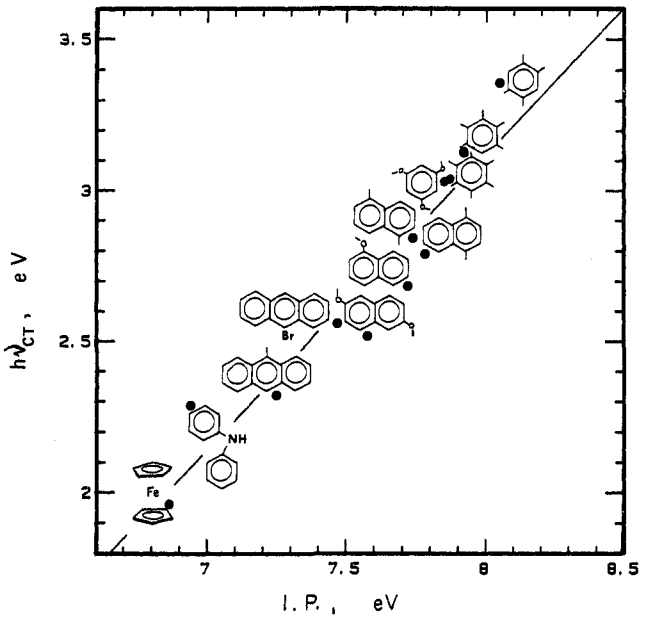

Figure 10. Mulliken correlation of the charge-transfer transition energy ($h\nu_{CT}$) with the ionization potential (IP) of the ferrocene and arene donors in $(DUR)_2Fe^{2+}$ complexes. The line is arbitrarily drawn with a slope of unity.

upon the dication reduction. The rate of deligation was related to the lifetime of the monocation,[56] as qualitatively evaluated in Table IV by the minimum scan rate (v_{min}) sufficient to achieve electrochemical reversibility of the first cyclic voltammetric wave P_1.

Discussion

Bis(arene)iron(II) dications $(Ar)_2Fe^{2+}$ can effectively serve as electron acceptors in the facile formation of various types of weak charge-transfer complexes, as spectrally detected in solution by the spontaneous appearance of new visible absorption bands. The linear correlation shown in Figure 10, arbitrarily drawn with a slope of unity, confirms the charge-transfer absorption ($h\nu_{CT}$) to apply equally to such structurally diverse donors as ferrocene and the various arenes (Table I)[57] according to the Mulliken formulation,[17] i.e.

$$h\nu_{CT} = IP - EA - \omega \qquad (9)$$

when the electron affinity (EA) of the bis(durene)iron(II) acceptor and the work term (ω) are constant.[58] Most importantly, the successful isolation of single crystals of the 1:1 molecular complexes with ferrocene as well as electron-rich arenes (see the Experimental Section) allows X-ray crystallography to identify the relevant charge-transfer interactions of the bis(arene)iron(II) acceptor with both of these structurally divergent electron donors, as described below.

Chart I. Orbital Correlation of Ferrocene[63]

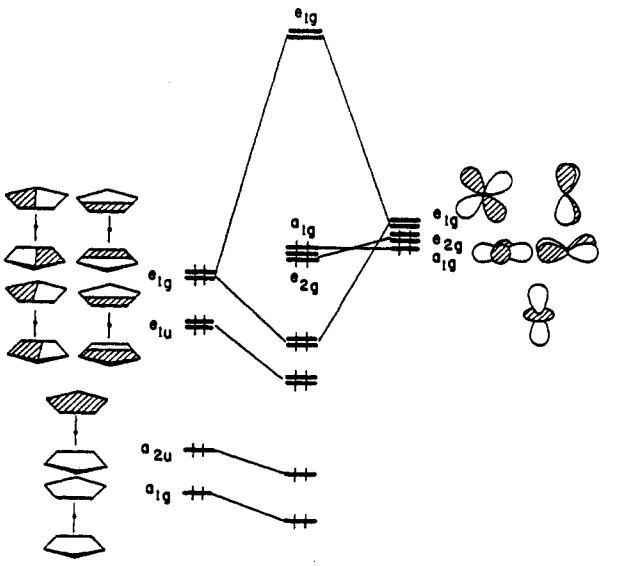

Charge-Transfer Structures of Bis(arene)iron(II) Acceptors with Ferrocene and Arene Donors. Ferrocene yields a series of molecular complexes with the bis(arene)iron(II) dications that are characterized in acetonitrile solution by the appearance of charge-transfer absorption bands in the visible spectrum between 600 and 800 nm. With the hexamethylbenzene derivative $(HMB)_2Fe^{2+}$, a very dark, almost black 1:1 crystalline complex with λ_{CT} = 626 nm is obtained from acetonitrile solutions. This compares with the green 1:1 complex of ferrocene with tetracyanoethylene that exhibits its charge-transfer absorption at 900 and 1075 nm in cyclohexane solution.[9] The ORTEP diagram of the tetragonal unit cell of $[Cp_2Fe, (DUR)_2Fe^{2+}(PF_6^-)_2]$ in Figure 3 shows the vertical stackings of alternate donor–acceptor pairs—each derived from the intact ferrocene donor and bis(arene)iron(II) acceptor. Indeed, we believe that such a heterosoric stack of more or less homomorphous donor and acceptor units is ideally constituted to access an interesting class of novel organometallic ferromagnets.[59,60] Be that now as it may, the location of the ferrocene donor poised over the bis(arene)iron(II) acceptor is consistent with the charge-transfer interaction in the molecular complex occurring principally via the contiguous placement of cyclopentadienyl and arene ligands on the donor and acceptor, respectively. Indeed, the intimate van der Waals contact of these coplanar ligands, with coincident (quasi) C_5 and C_6 axes, optimizes the overlap of the filled cyclopentadienyl π-orbital with the vacant e_{1g} arene orbital. However such an orbital correlation of charge transfer in this pair of sandwich structures does not represent the usual HOMO–LUMO transition in other molecular complexes.[61] Thus, the interaction diagram (Chart I) of ferrocene [and also applicable to bis(arene)iron(II) with equivalent orbital topology] identifies a set of three close-lying HOMOs centered on iron.[62]

The charge transfer from the subjacent ligand π-orbital of the ferrocene donor to the bis(arene)iron(II) acceptor is analogous to that previously presented in the ferrocene complex with the

(56) The increasing lifetimes of the 19-electron radical ion bis(arene)-iron(1) in the order $(MES)_2Fe^+ \sim (DUR)_2Fe^+ \ll (HMB)_2Fe^+$ follow the ligand donicity. For related examples, see: (a) Astruc, D. *Tetrahedron* **1983**, *39*, 4027. (b) Michaud, P.; Astruc, D.; Ammeter, J. H. *J. Am. Chem. Soc.* **1982**, *104*, 3755. (c) Darchen, A. *J. Chem. Soc., Chem. Commun.* **1983**, 768. (d) Nesmeyanov, A. N.; Vol'kenau, N. A.; Shilovtseva, L. S.; Petrakova, V. A. *J. Organomet. Chem.* **1973**, *61*, 329. (e) Moinet, C.; Roman, E.; Astruc, D. J. *Electroanal. Chem.* **1981**, *121*, 241. (f) Hamon, J.-R.; Astruc, D.; Michaud, P. *J. Am. Chem. Soc.* **1981**, *103*, 758.

(57) For the arene ionization potentials in Table I, see the following. (a) Methylbenzenes: Howell et al. in ref 29. (b) 1,3,5-Trimethoxybenzene, estimated from E° = 1.49 V vs SCE: Zweig, A.; Hodgson, W. G.; Jura, W. H. *J. Am. Chem. Soc.* **1964**, *86*, 4124. (c) 2,6-Dimethoxynaphthalene: Nagy, O. S.; Dupire, S.; Nagy, J. B. *Tetrahedron* **1975**, *31*, 2453. (d) Anthracenes: Masnovi, J. M.; Seddon, E. A.; Kochi, J. K. *Can. J. Chem.* **1984**, *62*, 2552. (e) 1,4-Dimethylnaphthalene: Nounou, P. *J. Chim. Phys.* **1966**, *63*, 994. (f) Diphenylamine: Godik, V. A.; Rodionov, A. N.; Shigorin, D. N. *Russ. J. Phys. Chem. (Eng. Transl.)* **1988**, *62*, 481. (g) 1,5-Dimethylnaphthalene: Aladekomo, J. B.; Birks, J. B. *Proc. R. Soc. A.* **1965**, *284*, 551. (h) 1-Methoxynaphthalene: Bock, H.; Wagner, G.; Kroner, J. *Chem. Ber.* **1972**, *105*, 3850.

(58) See: Kochi, J. K. *Angew. Chem., Int. Ed. Engl.* **1988**, *27*, 1227.

(59) For the heterosoric stacking in charge-transfer crystals, see: Wright, J. D. *Molecular Crystals*; Cambridge University Press: Cambridge, 1987.

(60) Miller, J. S.; Epstein, A. J. *Philos. Trans. R. Soc. London* **1990**, *A330*, 205. See also: Miller, J. S.; Epstein, A. J. *Adv. Chem. Ser.* **1990**, *No. 226*, 419 ff.

(61) (a) Prout, C. K.; Kamenar, B. *Molecular Complexes*; Foster, R., Ed.; Crane, Russak & Co.: New York, 1973; Vol. I, pp 151 ff. (b) Herbstein, F. H. In *Perspectives in Structural Chemistry*; Ibers, J. A., Ed.; Wiley: New York, 1971; pp 166 ff.

(62) Green, J. C. *Struct. Bonding (Berlin)* **1981**, *43*, 37.

(63) Albright, T. A.; Burdett, J. K.; Whangbo, M. H. *Orbital Interactions in Chemistry*; Wiley: New York, 1985. We thank T. A. Albright for helpful discussions and kindly permitting this reproduction.

π-acceptor tetracyanoethylene.[64] Basically the same charge-transfer formulation is therefore applicable to the structural situation with the reverse polarity, namely, that found in the charge-transfer complex of the bis(arene)iron(II) acceptor with the arene π-donor shown in Figure 5. The alternative HOMO–LUMO interaction stemming from the iron-centered orbitals is structurally provided by the side-by-side placement of the ferrocene donor and bis(arene)iron(II) acceptor, as shown in Figure 4 by the nonbonded Fe–Fe separation of 7.92 Å between the heterosoric stacks. Although this intermolecular separation is only slightly greater than the iron-to-iron distance of 6.64 Å within the stack, the HOMO–LUMO transition does not provide a consistent formulation for the structures of the [ferrocene–TCNE] and [arene–bis(arene)iron(II)] complexes, in which the possibility of such an orbital correlation does not exist. On the other hand, charge-transfer transitions involving the subjacent orbitals as described above provide the unifying formulation for all the ferrocene and bis(arene)iron(II) complexes in which the proximal juxtapositions of ligand π-orbitals are unmistakable.

Charge-Transfer Deligation of the Bis(arene)iron(II) Complexes with Ferrocene and Arene Donors. Photoactivation of the bis(arene)iron(II) complexes with ferrocene and arene donors (D) by the selective irradiation of the charge-transfer absorption bands shown in Figures 1 and 4 uniformly results in the deligation of the acceptor moiety according to the stoichiometry in eqs 5 and 6, respectively. Time-resolved picosecond spectroscopy establishes the transient cation radical of the donor (i.e., $D^{\cdot+}$) to be the spectral feature that both complexes share in common upon charge-transfer excitation ($h\nu_{CT}$). Thus, the fleeting appearance of the oxidized donors, ferrocenium ion (Cp_2Fe^+) in Figure 7 and 9-methylanthracene cation radical ($MeAn^{\cdot+}$) in Figure 8, immediately following the application of the 18-ps laser pulse is in accord with the Mulliken formulation of the CT photoactivation of the molecular complexes, viz

$$[CpFe, Ar_2Fe^{2+}] \xrightarrow{h\nu_{CT}} [Cp_2Fe^+, Ar_2Fe^+] \qquad (10)$$

and

$$[MeAn, Ar_2Fe^{2+}] \xrightarrow{h\nu_{CT}} [MeAn^{\cdot+}, Ar_2Fe^+] \qquad (11)$$

in which the reduced acceptor Ar_2Fe^+ is a common partner.[51,65] Since the transient electrochemical studies of bis(arene)iron(II) reduction in Figure 9 and Table IV identify the rapid fragmentation of Ar_2Fe^+ according to eq 8, the charge-transfer deligation can be most economically formulated as

Scheme I

$$Ar_2Fe^{2+} + D \rightleftharpoons [D, Ar_2Fe^{2+}] \qquad (12)$$

$$[D, Ar_2Fe^{2+}] \underset{k_{-1}}{\overset{h\nu_{CT}}{\rightleftharpoons}} [D^{\cdot+}, Ar_2Fe^+] \qquad (13)$$

$$[D^{\cdot+}, Ar_2Fe^+] \xrightarrow{k_1} [D^{\cdot+}, 2Ar, Fe^+] \qquad (14)$$

$$[D^{\cdot+}, 2Ar, Fe^+] \xrightarrow{\text{fast}} D + 2Ar + Fe^{2+} \qquad (15)$$

According to Scheme I, the photochemical process proceeds from the selective excitation of the molecular complex to the charge-transfer ion pair in eq 13. As such, the fragmentation (k_1) of the labile moiety Ar_2Fe^+ in eq 14 leads to the deligation of the acceptor.[55,56] The overall photoefficiency of the process would be largely determined by the competition between the fragmentation (k_1) and back electron transfer (k_{-1}).

The mechanism in Scheme I is indeed consistent with the various experimental facets of charge-transfer deligation. For example, the photoefficiency of charge-transfer deligation, as

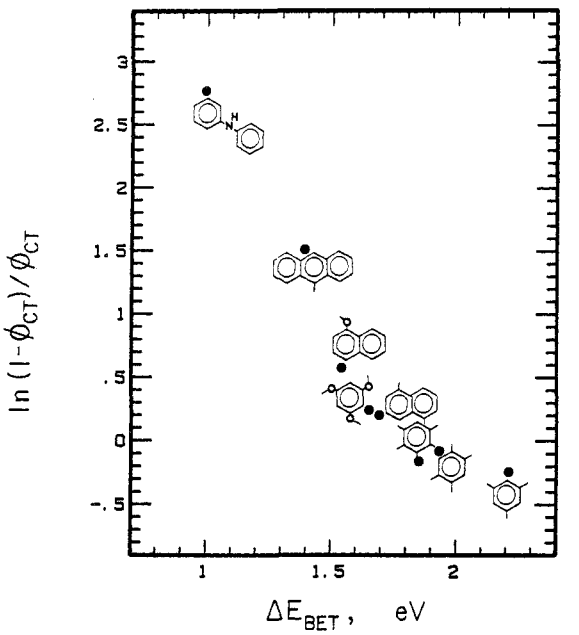

Figure 11. Variation of the photoefficiency for charge-transfer deligation with the driving force for back electron transfer according to eq 19.

measured by the quantum yield, relates directly to the ratio of rate constants in Scheme I, i.e.[66]

$$\phi_{CT} = k_1/(k_1 + k_{-1}) \qquad (16)$$

Thus, in the MeAn-induced deligation, the trend in the quantum yields for $(DUR)_2Fe^{2+} > (HMB)_2Fe^{2+}$, as listed in Table III, follows predictably from the lifetimes (k_1^{-1}) of the labile monocations $(DUR)_2Fe^+ < (HMB)_2Fe^+$, as evaluated by the relative values of v_{min} in Table IV from the transient electrochemical studies.[56] Furthermore, the remarkable trends in Table III for the quantum yields to decrease with the increasing strength of the arene donor must take specific cognizance of the rate of back electron transfer (k_{-1}). Since the latter results in the annihilation of the ion pair $Ar_2Fe^+/D^{\cdot+}$, it is readily evaluated from the separate redox couples, i.e.

$$Ar_2Fe^{2+} + e \underset{}{\overset{E^\circ_{red}}{\rightleftharpoons}} Ar_2Fe^+ \qquad (17)$$

$$D \underset{}{\overset{E^\circ_{ox}}{\rightleftharpoons}} D^{\cdot+} + e \qquad (18)$$

by the driving force $-\Delta G_{BET} = \mathcal{F}\Delta E_{BET}$ where $\Delta E_{BET} = -(E^\circ_{ox} + E^\circ_{red})$ and $\mathcal{F}$ is the faraday constant. Based on the linear free energy relationship,[68] $-\Delta G_{BET} = (RT/\alpha) \ln k_{-1} + \text{constant}$ (α is

(64) Adman, E.; Rosenblum, M.; Sullivan, S.; Margulis, T. N. *J. Am. Chem. Soc.* **1967**, *89*, 4540.

(65) The transient spectrum appearing in Figure 7 as a broad envelope suggests it to be a composite spectrum of Cp_2Fe^+ and $(HMB)_2Fe^+$, as described by Wilkinson et al. in ref 42 and Fischer et al. in ref. 44, respectively.

(66) Charge-transfer excitation to the ion radical pair in eq 13 is expected to occur with photoefficiencies approaching unity.[67]

(67) See: Kochi, J. K. *Acta Chem. Scand.* **1990**, *44*, 409.

(68) Hammett, L. P. *Physical Organic Chemistry*; second ed.; McGraw-Hill: New York, 1970; pp 348 ff. The use of the linear free energy relationship (LFER) is based on recent femtosecond/picosecond studies (Asahi, T.; Mataga, N. *J. Phys. Chem.* **1989**, *93*, 6575), which identify the charge recombination rates of geminate ion pairs formed by the photoexcitation of CT complexes to follow a linear dependence on the energy gap. Such a free energy relationship differs from back electron transfer rates of ion pairs formed by diffusional encounters in fluorescence quenching that follow the quadratic relationship (Marcus) (see, e.g., Ohno, T.; Yoshimura, A.; Mataga, N. *J. Phys. Chem.* **1990**, *94*, 4871.) For further studies of charge separation in the excited state of CT complexes, see: Ojima, S.; Miyasaka, H.; Mataga, N. *J. Phys. Chem.* **1990**, *94*, 4147, and related papers.

(69) Values of E°_{ox} estimated for the following. (a) Methylbenzenes: Howell et al.[29] converted to SCE (−0.24 V) and corrected for solvent change (−0.06 V). (b) 1,5-Dimethylnaphthalene, estimated from E°_{ox} of 1,4-isomer (1.51 V): Sankararaman, S., unpublished results. (c) 1,3,5-Trimethoxybenzene: Zweig, A. in ref 57b. (d) 1-Methoxynaphthalene: Zweig, A.; Maurer, A. H.; Roberts, B. G. *J. Org. Chem.* **1967**, *32*, 1322. (e) Anthracenes: Masnovi et al. in ref 57d. (f) Diphenylamine and *N,N*-dimethylaniline: Dvorak, V.; Nemec, I.; Zy'ka, J. *Microchem. J.* **1967**, *12*, 99. (g) *N*-Methylacridane: Hapiot, P.; Moiroux, J.; Saveant, J. M. *J. Am. Chem. Soc.* **1990**, *112*, 1337. (h) Ferrocene: Stolzenberg et al. in ref 2.

Table V. Driving Force for Back Electron Transfer ($-\Delta G_{BET}$) of Charge-Transfer Ion Pairs from Bis(arene)iron(II) Complexes with Ferrocene and Arene Donors[a]

donor	$-E^\circ_{ox}$,[b] V	$-\Delta G_{BET}$ (kcal mol^{-1}) for $(Ar)_2Fe^{2+}$[c] BZ	MES	DUR	HMB
benzene	2.40	55	57	59	61
mesitylene	2.05	47	49	51	53
durene	1.77	41	42	45	47
pentamethylbenzene	1.69	39	40	43	45
hexamethylbenzene	1.56	36	37	40	42
1,5-dimethylnaphthalene	1.53	35	36	39	41
1,3,5-trimethoxybenzene	1.49	34	36	38	40
1-methoxynaphthalene	1.38	32	33	36	38
9-bromoanthracene	1.38	32	33	36	38
2,6-dimethoxynaphthalene	1.33	30	32	34	36
9-methylanthracene	1.23	28	30	31	34
N-methylacridane	0.86	20	21	24	26
diphenylamine	0.83	19	21	23	25
N,N-dimethylaniline	0.68	15	17	19	22
ferrocene	0.41	9	11	13	15

[a] In acetonitrile solution at 25 °C. [b] Relative to SCE, from ref 69. [c] E°_{red} = −0.06, −0.16, and −0.26 V vs SCE for MES, DUR, and HMB derivatives of Ar_2Fe^{2+}; E°_{red} = 0.01 for BZ derivative estimated from Table I.

the **Brønsted** coefficient), the photoefficiency in eq 16 can be reexpressed as

$$\Delta E_{BET} = RT/\alpha\mathcal{F}\ [\ln\ (1 - \phi_{CT})/\phi_{CT} + \ln\ k_1] + \text{constant} \qquad (19)$$

Indeed, the monotonic trend observed in Figure 11 for the quantum yield data in Table III represents strong support for the mechanism in Scheme I, since ln k_1 is invariant for a given bis(arene)iron(II) acceptor.[70] The listings for the various arene donors in Table V show the driving force for back electron transfer to be highly exergonic (40–60 kcal mol^{-1}). It is noteworthy that such large magnitudes of $-\Delta G_{BET}$ are likely to lie in the Marcus inverted region of the free energy relationship for electron transfer.[71-73] The net result is an increase in the rate of back electron transfer with increasing donor strength.[74]

Comments on the Thermal Deligation of Charge-Transfer Complexes of Bis(arene)iron(II) Acceptors. The majority of the charge-transfer complexes of the bis(arene)iron(II) acceptors examined in this study persist for prolonged periods—provided the solutions are protected from light, even adventitious room light. However, in some instances, the bis(arene)iron(II) complexes react spontaneously in the dark. For example, the characteristically broad charge-transfer band from the mesitylene dication $(MES)_2Fe^{2+}$ and ferrocene (compare Figure 1) is fleeting, and it disappears in less than 15 min after the solutions are mixed. The resultant spectrum shows a residual absorbance centered at 620 nm, which is diagnostic of the ferrocenium ion.[42] By way of contrast, the weaker acceptors $(DUR)_2Fe^{2+}$ and $(HMB)_2Fe^{2+}$ produce charge-transfer complexes that are persistent for prolonged periods under the same dark conditions. In an analogous manner, the solutions of the charge-transfer complexes of $(DUR)_2Fe^{2+}$ with such strong amine donors as *N*-methylacridane and *N,N*-dimethylaniline upon standing in the dark liberate durene with essentially the same stoichiometry as that given in eq 6.

The dark reactions derive from the charge-transfer complexes that clearly involve the most electron-rich donors and electron-poor acceptors, as judged by their oxidation and reduction potentials in Table V. The inspection of Table V thus reveals that the driving force for electron transfer between the bis(arene)iron(II) acceptor and the various donors, when evaluated as $-\Delta G_{ET} = \mathcal{F}(E^\circ_{ox} + E^\circ_{red})$, is the largest for ferrocene, *N*-methylacridane, and *N,N*-dimethylaniline, especially when those strong donors are paired with the electron-poor MES derivative of the bis(arene)iron(II) acceptor.[75] As such, we tentatively propose that the dark reactions arise via essentially the same multistep mechanism as that proposed in Scheme I for charge-transfer deligation—the difference arising from an adiabatic electron transfer, e.g.

$$[Cp_2Fe, (MES)_2Fe^{2+}] \xrightarrow{\Delta} [Cp_2Fe^+, (MES)_2Fe^+], \text{ etc.} \qquad (20)$$

that is thermally allowed when the driving force $-\Delta G_{ET}$ is sufficient to surmount the barrier that is otherwise overcome by charge-transfer activation in eq 13. Such a conclusion provides a relevant link to the unifying theme for the photochemical and thermal activations of electron transfer in various other organometallic processes.[67]

Experimental Section

Materials. The arene donors were obtained as commercial samples, and they were recrystallized prior to use (solvent): durene and pentamethylbenzene (Aldrich, ethanol/benzene), hexamethylbenzene (Fluka, ethanol), 9-methyl- and 9,10-dimethylanthracene (Aldrich, ethanol), and diphenylamine (Baker, ethanol/water); otherwise 1,3,5-trimethoxybenzene (Aldrich), 1-methoxynaphthalene (Aldrich), 1,5-dimethylnaphthalene (Aldrich), and 9-bromoanthracene (Aldrich) were used as received. The bis(arene)iron(II) acceptors were prepared as the crystalline hexafluorophosphate salts by the treatment of the appropriate arene (benzene, mesitylene, or durene) with anhydrous ferric chloride (Pennwalt) and aluminum chloride (Fluka) according to the literature procedure.[76,77] The hexamethylbenzene derivative $(HMB)_2Fe^{2+}(PF_6^-)_2$ was prepared from ferrous chloride, aluminum chloride, and hexamethylbenzene by an analogous procedure.[77] Acetonitrile (Mallinckrodt, reagent) was stirred with 1% $KMnO_4$ for 24 h. After being heated under reflux for an additional hour, the mixture was filtered and then successively redistilled from P_2O_5 and CaH_2 under an argon atmosphere. Acetone (Baker, reagent) was distilled from $CaSO_4$ under argon.

Instrumentation. UV–vis spectra were recorded on a Hewlett–Packard 8450A diode-array spectrometer with 2-nm resolution. ^1H NMR spectra were obtained on a JEOL FX90Q spectrometer and chemical shifts are reported in ppm downfield from the internal TMS standard. Electrochemical measurements were carried out with 5×10^{-3} M bis(arene)-iron(II) salts in acetonitrile containing 0.1 M tetra-*n*-butylammonium hexafluorophosphate (TBAH) as the supporting electrolyte. Cyclic voltammetry was performed on a Bioanalytical System 100A electrochemical analyzer using a conventional three-electrode cell. A platinum disk electrode served as the working electrode that was referenced to an aqueous SCE standard electrode. Steady-state photolyses were carried out with the focused beam of an Osram (XBO) 450-W xenon lamp. The light was passed through an aqueous IR filter and either a Pyrex sharp-cutoff filter (Corning CS-3 series) or an interference filter (Ditric Optics, fwhm ± 5 nm).

Determination of the Formation Constant of Bis(arene)iron(II) Complexes. Typically a solution of 6.0×10^{-3} M $(MES)_2Fe^{2+}(PF_6^-)_2$ in 5 mL of acetonitrile was incrementally treated in the dark with weighed amounts (20 mg) of 9-methylanthracene, and the absorbance (A) change at 532 nm was measured. By the Benesi–Hildebrand procedure,[36] the linear plot of $[(MES)_2Fe^{2+}]/A$ vs $[MeAn^{-1}]$ yielded a slope of $(K\epsilon')^{-1}$ = 1.08 and an intercept of $(\epsilon')^{-1} = 2.6 \times 10^{-3}$. The values of K = 2.5 M^{-1} and ϵ = 400 M^{-1} cm^{-1} represented an upper limit owing to competition

(70) The linear relationship in Figure 11 has a slope of −2.6 eV^{-1}, but with a correlation coefficient of 0.94. However, it is important to emphasize that the linear free energy relationship for the evaluation of K_{-1} is an approximation. See footnote 74.

(71) Marcus, R. A. *J. Chem. Phys.* **1956**, *24*, 966; Marcus, R. A. *Discuss. Faraday Soc.* **1960**, *29*, 21.

(72) For experimental support, see: Closs, G. L.; Miller, J. R. *Science* **1988**, *240*, 440.

(73) For the observation of the Marcus inverted region in the back electron transfer from charge-transfer ion pairs, see: Gould, I. R.; Moody, R.; Farid, S. *J. Am. Chem. Soc.* **1988**, *110*, 7242.

(74) This leads to the negative Brønsted slope in the linear free energy relationship (vide supra). A similar LFER was observed in the "inverted" rates of back electron transfer from charge-transfer ion pairs by Asahi and Mataga.[68] See also: Reference 73. The distinction between the Marcus equation and the LFER to describe back electron transfer probably relates to the difference between outer-sphere and inner-sphere processes,[67] respectively.

(75) The use of the E° values in Table V for back electron transfer necessitates a change in sign for the driving force for electron transfer.

(76) (a) Helling, J. F.; Rice, S. L.; Braitsch, D. M.; Mayer, T. *J. Chem. Soc., Chem. Commun.* **1971**, 930. (b) Helling, J. F.; Braitsch, D. M. *J. Am. Chem. Soc.* **1970**, *92*, 7207. (c) Mandon, D.; Astruc, D. *J. Organomet. Chem.* **1989**, *369*, 383. See also: Fischer, E. O.; Böttcher, R. *Chem. Ber.* **1956**, *89*, 2397.

(77) For a discussion of whether the CT complex is (or is not) an intermediate in the thermal processes, see footnote 69 in: Fukuzumi, S.; Kochi, J. K. *J. Am. Chem. Soc.* **1980**, *102*, 2141.

from a slow decomposition. The attempted determination of K for other CT pairs such as $(BZ)_2Fe^{2+}$/MeAn and $(MES)_2Fe^{2+}$/mesitylene was adversely affected by either decomposition or low formation constants. Although the low solubilities prevented the accurate measurement of the formation constants of the ferrocene complexes, they were judged generally to be weak, with K comparable to those of the arene complexes.

Crystallization of Bis(arene)iron(II) Complexes with Ferrocene and Arenes. To a solution of 98 mg (0.16 mmol) of $(DUR)_2Fe^{2+}(PF_6^-)_2$ in 3 mL of acetonitrile was added a solution of ferrocene (68 mg, 0.38 mmol) in 3 mL of acetonitrile. The slow addition of 3 mL of THF to the yellow-brown solution yielded 56 mg (0.07 mmol, 44%) of a dark brown, almost black microcrystalline precipitate. Dissolution of the crystals in acetonitrile afforded a dark brown solution, the ^1H NMR spectra of which indicated the presence of an equimolar ratio of ferrocene and $(DUR)_2Fe^{2+}$. Octahedral crystals of the charge-transfer complex suitable for X-ray crystallography (vide infra) were obtained by the slow diffusive mixing of more concentrated (0.1 M) solutions. Anal. Calcd for $C_{30}H_{38}F_{12}P_2Fe$: C, 45.02; H, 4.79. Found: C, 45.05; H, 4.81. The 1:1 complex of $(HMB)_2Fe^{2+}(PF_6^-)_2$ and ferrocene was similarly obtained in 47% yield. For the arene donors, typically a solution of 100 mg of $(HMB)_2Fe^{2+}(PF_6^-)_2$ in 2 mL of acetone was carefully overlaid with a saturated solution of the arene in 2 mL of acetone. Thus, bright orange crystals of the 1:1 complex with durene separated upon standing in the dark, and they were mounted for X-ray crystallography. Spectral (^1H and ^{13}C NMR) analysis indicated a 1:1 ratio of durene and $(HMB)_2Fe^{2+}$, together with acetone of crystallization. Although the volatile nature of the latter precluded a reliable elemental analysis, X-ray analysis of the epoxy-coated crystal revealed the presence of acetone solvate (vide infra). Analogously, the charge-transfer complexes of $(HMB)_2Fe^{2+}(PF_6^-)_2$ with 9-methylanthracene and 9,10-dimethylanthracene were obtained from acetone solution. Diphenylamine formed dark purple needles of the 1:2 complex with $(HMB)_2Fe^{2+}(PF_6^-)_2$. Anal. Calcd for $C_{60}H_{83}F_{24}NP_4Fe_2$: C, 47.73; H, 5.54; N, 0.93. Found: C, 48.04; H, 5.63, N, 1.06. Spectral (^1H and ^{13}C NMR) examination of the solutions prior to crystallization always indicated the composite spectrum of each component. No evidence for salt formation was found.

Photochemistry of the Bis(arene)iron(II) Complexes with Ferrocene and Arene Donors. Charge-transfer deligation of the bis(arene)iron(II) acceptor was readily determined under an argon atmosphere by following the change in the ^1H NMR spectrum for the coordinated ligand [typically, $(BZ)_2Fe^{2+}$ δ 6.95 (s); $(MES)_2Fe^{2+}$ δ 6.45 (s, 6 H) and 2.54 (s, 18 H); $(DUR)_2Fe^{2+}$ δ 6.45 (s, 4 H) and 2.42 (s, 24 H); and $(HMB)_2Fe^{2+}$ δ 2.25 (s)] to the ^1H NMR spectrum of the free arene [BZ δ 7.30; MES δ 6.80 and 2.21; DUR δ 6.89 and 2.18; and HMB δ 2.20], using the internal standard (CH_3NO_2) method for quantitative analysis. As a reliability check, the same changes were also determined by the downfield shifts in the corresponding ^{13}C NMR spectra, e.g., $(MES)_2Fe^{2+}$ δ 91.6 and 19.7 to free mesitylene δ 138.4, 127.3, and 20.7; $(DUR)_2Fe^{2+}$ δ 108.4, 95.1, and 17.7 to free durene δ 134.2, 131.5 and 18.8; $(HMB)_2Fe^{2+}$ δ 104.6 and 16.3 to free hexamethylbenzene δ 16.7. The amount of iron liberated was determined by complexation with 2,2′-bipyridine followed by the spectrophotometric determination of the resultant $Fe(bipy)_3^{2+}$ at λ 520 nm with $\epsilon = 8560$ M^{-1} cm^{-1} in a solution of aqueous acetonitrile (80/20 v/v).[40] Control experiments were always carried out to establish that no deligation of the bis(arene)iron(II) occurred in the dark.[31]

The quantum yields were determined by Reineckate actinometry with $K[Cr(NCS)_4(NH_3)_2]$ according to the procedure of Wegner and Adamson.[78] For the charge-transfer deligation of the $(DUR)_2Fe^{2+}$ complex with 9-methylanthracene carried out at $\lambda_{exc} = 620$ nm, the quantum yield ϕ_{CT} was obtained from the linear plots based on the transmittance change given as $\phi_{CT}\varphi t = m_0/\log T_0$ [log $(1 - 1/T)/(1 - 1/T_0)$] for the incident light flux φ within the time interval t for the solution originally containing m_0 moles of $(DUR)_2Fe^{2+}$ and showing the initial and final transmittance of T_0 and T, respectively. [Note that this relationship represents the integrated form of $dC/dt = -\Phi\varphi\ (1 - T)/V$, where C and V are the concentration and volume of the photolysate.] The quantum yields were independent of the flux variation between $\varphi = 2.5 \times 10^{-7}$ and 1.0×10^{-6} einsteins min^{-1}. Inspection of Figure 4 showed that CT excitations at shorter wavelengths were complicated by the overlapping spectrum of the bis(arene)iron(II) acceptor. Since the latter was also subject to a photoinduced substitution (vide infra), the charge-transfer quantum yield ϕ_{CT} was related to the observed quantum yield ϕ as $A_{CT}\phi_{CT}/A + A_{fe}\phi_{fe}/A = \phi$, where the subscripts CT and fe refer to the charge-transfer complex and bis(arene)iron(II), respectively, and A represents absorbance. The same additivity relationship more conveniently expressed in terms of the relative absorbances $a_{fe} = A_{fe}/A$ and $a_{CT} = A_{CT}/A$, can be rewritten as $\phi_{CT}/\phi_{fe} = (1 - a_{fe})^{-1}(\phi/\phi_{fe} - a_{fe})$. The quantum yield ϕ_{fe} was independently determined in the absence of viable donor (vide infra). [Benzene was added as the control since it did not give rise to a CT absorbance with $(DUR)_2Fe^{2+}$ at λ_{exc}.] In order to establish the reliability of the method, the charge-transfer deligation of the $(DUR)_2Fe^{2+}$ complex with 9-methylanthracene was examined at various wavelengths to encompass the CT band—from the red edge (620 nm) at which no spectral overlap occurred to the blue edge (460 nm) at which there was severe overlap (see Figure 4A). Since the results in the last column of Table II confirm the constancy of the charge-transfer quantum yield, the same method was used to determine ϕ_{CT} for the other bis(arene)iron(II) complexes. In Table II, $\phi_{fe}^* = a_{fe}\phi_{fe}$, $\phi_{CT}^* = \phi_{obs} - \phi_{fe}^*$, and $\phi_{CT} = \phi_{CT}^* a_{CT}^{-1}$. Thus, the quantum yields in Table III were determined at 440 nm with the various arenes in the order arene, M; $(DUR)_2Fe^{2+}$, M; ϕ/ϕ_{fe}; a_{fe}, %; a_{CT}, %; ϕ_{CT}/ϕ_{fe}; ϕ_{CT}. (1) Mesitylene, 0.96; 7.1×10^{-3}; 0.94; 76; 24; 0.74; 0.56. (2) Durene, 0.68; 4.9×10^{-3}; 0.86; 55; 45; 0.68; 0.52. (3) Pentamethylbenzene, 0.69; 4.6×10^{-3}; 0.85; 48, 52; 0.71; 0.54. (4) 1,3,5-Trimethoxybenzene, 0.35; 5.7×10^{-3}; 0.76; 43; 57; 0.58; 0.44. (5) 1,5-Dimethylnaphthalene, 0.40; 6.6×10^{-3}; 0.75; 39; 61; 0.59; 0.45. (6) 1-Methoxynaphthalene, 0.49; 1.6×10^{-3}; 0.64; 32; 68; 0.47; 0.36. (7) 9-Methylanthracene (at 500 nm), 0.15; 5.1×10^{-3}; 0.45; 27; 73; 0.24; 0.18.

The photoinduced deligation of bis(arene)iron(II) was examined separately in acetonitrile solution. For example, the actinic irradiation of a solution (varying in concentration from 0.003 to 0.01 M) for $(DUR)_2Fe^{2+}$ in acetonitrile at 440 nm yielded free durene and ferrous ion in a 2:1 molar ratio. Thus, the net photoreaction involved the replacement of arene ligands with acetonitrile similar to the charge-transfer deligations in eqs 5 and 6. The photoefficiencies at various excitation wavelengths were as follows (λ_{exc}, Φ): 400, 0.71; 440, 0.76; 440 (plus 0.1 M TBAH), 0.76; 440 (plus 1.3 M benzene), 0.76; 480, 0.78; 500, 0.78; 540, 0.85. The slight wavelength dependence of the quantum yield can be attributed to the varying degree of ligand character in the 2 e_{1g} and e_{2u} orbitals, which are populated by the pair of (visible) electronic transitions $a^1E_{1g} \leftarrow {}^1A_{1g}$ and $^1E_{2g} \leftarrow {}^1A_{1g}$ at 525 and 453 nm, respectively.[79,80] The variation in the efficiency of the photosubstitution for various derivatives induced at 540 nm were as follows (Ar_2Fe^{2+}, Φ): $(MES)_2Fe^{2+}$, 0.81; $(DUR)_2Fe^{2+}$, 0.85; $(HMB)_2Fe^{2+}$, 0.020 in 0.01 M acetonitrile solutions. These quantum yields were used as corrections for the establishment of the quantum yield for charge-transfer deligation of the complex (vide supra). The determination of the quantum yields for deligation of the bis(arene)iron(II) complexes with ferrocene was complicated by the residual absorbance due to small amounts of ferrocenium ion (λ_{max} = 615 nm),[42] together with that of an unknown component with a broad absorption between 680 and 800 nm (tentatively ascribed to colloidal iron[54]).

X-ray Crystallography of Bis(arene)iron(II) Complexes with Ferrocene and Arene Donors. A carmine fragment of [Cp_2Fe, $(DUR)_2Fe^{2+}(PF_6^-)_2$] having approximate dimensions 0.50 × 0.45 × 0.35 mm was cut from a large octahedron and mounted in a random orientation on a Nicolet R3m/V automatic diffractometer. The radiation used was Mo Kα monochromatized by a highly ordered graphite crystal. Final cell constants, as well as other information pertinent to data collection and refinement, were as follows: space group $P4_2/nmc$ (tetragonal); cell constants $a = 11.200$ (3) Å, $c = 13.283$ (5), $V = 1666$ Å^3; formula weight 800.32; formula units per cell $Z = 2$; density $\rho = 1.60$ g cm^{-3}; absorption coefficient $\mu = 10.51$ cm^{-1}; radiation (Mo Kα) $\lambda = 0.71073$ Å; collection range $4° \le 2\theta \le 50°$; scan width $\Delta\theta = 1.20 + (K\alpha_2 - K\alpha_1)°$; scan speed range 2.0–15.0° min^{-1}; total data collected 812; independent data $I > 3\sigma(I)$ 501, total variables 58; $R = \sum||F_o| - |F_c||/\sum|F_o|$ 0.073; $R_w = [\sum w(|F_o| - |F_c|)^2/\sum w|F_o|^2]^{1/2}$ 0.064; weights $w = \sigma(F)^{-2}$. The Laue symmetry was determined to be $4/mmm$, and (from the systematic absences noted) the space group was shown unambiguously to be $P4_2/nmc$. Intensities were measured by the θ scan technique, with the scan rate depending on the count obtained in rapid prescans of each reflection. Two standard reflections were monitored after every 2 h or every 100 data collected, and these showed no significant variation. During data reduction, Lorentz and polarization corrections were applied; however, no correction for absorption was made due to the small absorption coefficient. Since there were only two formula units in the unit cell, the structure was solved by placing the Fe atoms on $\bar{4}m2$ sites 2a and 2b. This site symmetry presupposed massive disorder of the ferrocene molecule, and the Cp ring was treated as an ideal rigid body, with each carbon and hydrogen atom having 25% occupancy. The remaining non-hydrogen atoms were located in subsequent difference Fourier syntheses. The methyl groups were treated as ideal rigid bodies and allowed to rotate freely. The anion was also found to be massively

(78) Wegner, E. E.; Adamson, A. W. *J. Am. Chem. Soc.* **1986**, *88*, 394. See also: Rabek, J. F. *Experimental Methods in Photochemistry and Photophysics*; Wiley: New York, 1982; Part 2, p 946.

(79) Morrison, W. H.; Ho, E. Y.; Hendrickson, D. N. *Inorg. Chem.* **1975**, *14*, 500.

(80) Clack, D. W.; Warren, K. D. *Inorg. Chim. Acta* **1978**, *30*, 251.

Table VI. Atomic Coordinates ($\times 10^4$) and Equivalent Isotropic Displacement Parameters ($Å^2 \times 10^3$) of [Cp_2Fe, $DUR_2Fe^{2+}(PF_6^-)_2$]

	x	y	z	U(eq)[a]
Fe(1)	7500	2500	2500	32 (1)
Fe(2)	7500	2500	7500	48 (1)
P(1)	2554 (43)	2526 (43)	1109 (27)	58 (2)
F(1)	1637	3221	446	120
F(2)	3472	1832	1771	120
F(3)	1741	2713	2049	120
F(4)	3368	2340	168	120
F(5)	3216	3720	1347	120
F(6)	1894	1333	870	120
P(2)	2506 (39)	2442 (36)	1217 (21)	58 (2)
F(7)	2918	1654	2122	120
F(8)	2095	3231	313	120
F(9)	1570	1474	919	120
F(10)	3443	3412	1515	120
F(11)	3452	1826	529	120
F(12)	1561	3059	1905	120
P(3)	2492 (33)	2504 (55)	1109 (24)	58 (2)
F(13)	3395	3476	749	120
F(14)	1589	1533	1468	120
F(15)	3046	2550	2186	120
F(16)	1939	2459	31	120
F(17)	3397	1507	808	120
F(18)	1588	3502	1409	120
C(1)	6853 (7)	3646 (7)	1300 (6)	40 (2)
C(2)	6239 (12)	2500	1320 (9)	50 (3)
C(3)	6158 (7)	4757 (7)	1294 (6)	58 (2)
C(4)	7193 (16)	3695 (24)	6327 (7)	60 (3)
C(5)	6377	2730	6245	60 (3)
C(6)	7047	1654	6202	60 (3)
C(7)	8277	1955	6257	60 (3)
C(8)	8367	3217	6334	60 (3)

[a] Equivalent isotropic U defined as one-third of the trace of the orthogonalized U_{ij} tensor.

disordered about a 2-mm site. Eventually, by use of ideal rigid body models, three different orientations of PF_6^- were identified (before site symmetry considerations). Each of these was refined independently with occupancy factors of 8.33% (1/12). Fixed isotropic temperature factors were used for the fluorine atoms. The centers of these anion models were not constrained and were refined to three slightly different locations. After all shift/esd ratios were less than 0.5, convergence was reached at the agreement factors listed above. No unusually high correlations were noted between any of the variables in the last cycle of full-matrix least-squares refinement; and the final difference density map showed a maximum peak of about 0.75 e $Å^{-3}$, located quite close to $P1$. All calculations were made using Nicolet's SHELXTL PLUS (1987) series of crystallographic programs to yield the final atomic coordinates listed in Table VI.

A reddish-orange prismatic block of the $(HMB)_2Fe^{2+}$ complex with durene having approximate dimensions 0.50 × 0.45 × 0.35 mm was mounted in a random orientation on a Nicolet R3m/V automatic diffractometer. The sample was immediately coated with a thin layer of epoxy in order to retard the loss of solvent since the crystals were known to decompose within a few minutes after removal from the mother liquor. The crystallographic data were as follows: space group $P\bar{1}$ (triclinic); cell constants a = 9.270 (4) Å, b = 11.040 (5), c = 12.130 (5), α = 71.72 (3)°, β = 67.30 (3), γ = 77.41 (3)°, V = 1081 $Å^3$; molecular formula $(C_{24}H_{36}Fe^{2+})$ $(2PF_6^-)(C_{10}H_{14})(2C_3H_6O)$; formula weight 920.81; formula units per cell Z = 1; density ρ = 1.41 g cm^{-3}; absorption coefficient μ = 5.03 cm^{-1}; radiation (Mo Kα) λ = 0.710 73 Å; collection range $4° \le 2\theta \le 50°$; scan width $\Delta\theta = 1.20 + (K\alpha_2 - K\alpha_1)°$; scan speed range 2.0–15.0° min^{-1}; total data collected 3804; independent data, $I > 3\sigma(I)$ 3241; total variables 313; $R = \sum||F_o| - |F_c||/\sum|F_o|$ 0.066; $R_w = [\sum w(|F_o| - |F_c|)^2/\sum w|F_o|^2]^{1/2}$ 0.058; weights $w = \sigma(F)^{-2}$. The Laue symmetry was determined to be $\bar{1}$, and the space group was shown to be either $P1$ or $P\bar{1}$. Intensities were measured by the θ scan technique, with the scan rate depending on the count obtained in rapid prescans of each reflection. Two standard reflections were monitored after every 2 h or every 100 data collected, and these showed a 15% decay over the course of the experiment. A normalization factor as a function of X-ray exposure time was applied to account for this change. Since each of the nonsolvent molecules in the compound was capable of inversion symmetry, space group $P\bar{1}$ was assumed from the outset. The structure was solved by placing the Fe atom on an inversion center. Remaining non-hydrogen atoms were located in subsequent difference Fourier syntheses. The asymmetric unit was found to consist of half dication and half durene

Table VII. Atomic Coordinates ($\times 10^4$) and Equivalent Isotropic Displacement Parameters ($Å^2 \times 10^3$) of [Durene, $(HMB)_2Fe^{2+}(PF_6^-)_2$]

	x	y	z	U(eq)[a]
Fe	5000	5000	5000	26 (1)
P	2429 (7)	2199 (6)	1044 (5)	55 (1)
F(1)	1942	3579	342	120 (12)
F(2)	2919	819	1746	122 (12)
F(3)	1834	2639	2263	114 (9)
F(4)	3026	1759	−177	180 (18)
F(5)	4096	2579	730	183 (15)
F(6)	764	1820	1357	141 (11)
P′	2351 (9)	2139 (7)	1017 (6)	55 (1)
F(1′)	1400	3452	627	115 (11)
F(2′)	3300	827	1406	144 (14)
F(3′)	952	1786	2253	292 (18)
F(4′)	3748	2493	−219	172 (14)
F(5′)	3064	2768	1649	161 (17)
F(6′)	1636	1511	385	168 (19)
P″	2592 (12)	2060 (10)	1014 (12)	55 (1)
F(1″)	1597	957	1949	130 (6)
F(2″)	3585	3164	81	130 (6)
F(3″)	4130	1192	1116	130 (6)
F(4″)	1053	2930	914	130 (6)
F(5″)	2469	2580	2109	130 (6)
F(6″)	2714	1542	−79	130 (6)
O	9146 (5)	3401 (5)	7423 (4)	69 (2)
C(1)	4313 (6)	3072 (5)	5712 (5)	35 (2)
C(2)	5859 (6)	3019 (5)	5715 (5)	39 (2)
C(3)	7058 (6)	3599 (5)	4611 (5)	36 (2)
C(4)	6700 (6)	4189 (5)	3523 (5)	36 (2)
C(5)	5145 (6)	4222 (5)	3528 (5)	38 (2)
C(6)	3950 (6)	3671 (5)	4619 (5)	35 (2)
C(7)	3062 (7)	2441 (6)	6853 (5)	56 (3)
C(8)	6274 (8)	2309 (6)	6855 (5)	58 (3)
C(9)	8701 (6)	3524 (6)	4584 (6)	56 (3)
C(10)	7999 (7)	4737 (6)	2345 (5)	56 (3)
C(11)	4780 (8)	4807 (6)	2328 (5)	60 (3)
C(12)	2342 (6)	3691 (6)	4595 (6)	53 (3)
C(13)	5581 (8)	−565 (5)	5933 (5)	51 (3)
C(14)	4015 (7)	−578 (5)	6181 (5)	50 (3)
C(15)	3386 (7)	−2 (5)	5213 (6)	52 (3)
C(16)	2950 (9)	−1207 (7)	7478 (6)	80 (4)
C(17)	1693 (7)	55 (7)	5423 (7)	75 (4)
C(18)	8702 (7)	2859 (6)	8516 (6)	54 (3)
C(19)	8840 (11)	1460 (7)	8953 (7)	110 (6)
C(20)	8035 (9)	3601 (7)	9473 (6)	88 (4)

[a] Equivalent isotropic U defined as one-third of the trace of the orthogonalized U_{ij} tensor.

(located on separate inversion centers), with one anion and one molecule of acetone solvent (located in general positions). After the usual sequence of isotropic and anisotropic refinement, all hydrogens were entered into ideal calculated positions and constrained to riding motion, with a single variable isotropic temperature factor for all of them. The methyl groups were treated as ideal rigid bodies and allowed to rotate freely. The anion was found to be massively disordered, and by employing ideal rigid body models, three different orientations of PF_6^- were identified. On the basis of analysis of the isotropic thermal motion, the separate models were refined independently with occupancy factors of 42%, 35%, and 23% for the P, P′, and P″ models, respectively. Eventually the fluorine atoms in the more populous P and P′ models were converted to anisotropic thermal motion, but fixed isotropic temperature factors were used for the fluorine atoms in P″. The centers of these anion models were not constrained, and refined to three slightly different locations. After all shift/esd ratios were less than 0.3 (except for those involving the rigid-body hydrogens), convergence was reached at the agreement factors listed above. The final difference density map showed a maximum peak of about 0.6 e $Å^{-3}$. Calculations were made with the aid of the Nicolet programs above, and the final atomic coordinates are listed in Table VII.

Time-Resolved Spectroscopy of Bis(arene)iron(II) Complexes with Ferrocene and Arene Donors. Solutions of the charge-transfer complexes were made up in 4 mL of acetonitrile to yield an optimum absorbance at 532 nm of unity as follows: $(HMB)_2Fe^{2+}(PF_6^-)_2$ (9.0 mg) and 9-methylanthracene (157 mg), $(DUR)_2Fe^{2+}$ (8.0 mg) and 9-methylanthracene (151 mg), and 56 mg Cp_2Fe (56 mg) and $(HMB)_2Fe^{2+}(PF_6^-)_2$ (60 mg). The time-resolved picosecond spectrum were obtained by flash photolysis using the frequency-doubled (KDP crystal) output at 532 nm of a Nd^{3+}:YAG Q-switched laser (Quantel 501C-10) with 18-ps

(fwhm) pulses. The white light (1:1 D_2O/H_2O) probe beam was detected by a dual diode array (Princeton Instruments DDA512) consisting of 512 elements as described elsewhere.[81] The transient spectra in Figures 7 and 8 were obtained by averaging 300-500 shots, and the system was calibrated relative to the transient spectrum of the anthracene cation radical.[82]

(81) Sankararaman, S.; Kochi, J. K. *J. Chem. Soc., Perkin Trans. 2*, in press.
(82) Compare: Mataga, N.; Shioyama, H.; Kanda, Y. *J. Phys. Chem.* **1987**, *91*, 314. See also: References 19 and 30.

Acknowledgment. We thank T. M. Bockman for providing critical ideas and suggestions, J. D. Korp for crystallographic assistance, Z. Karpinski for the electrochemical measurements, S. Sankararaman for the time-resolved spectra, and the National Science Foundation, Robert A. Welch Foundation, and the Texas Advanced Research Program for financial support.

Supplementary Material Available: Tables of the observed and calculated structure factors for $[Cp_2Fe, (DUR)_2Fe^{2+}(PF_6^-)_2]$ and [durene, $(HMB)_2Fe^{2+}(PF_6^-)_2$] (17 pages). Ordering information is given on any current masthead page.

Factors Determining the Site of Electroreduction in Nickel Metalloporphyrins. Spectral Characterization of Ni(I) Porphyrins, Ni(II) Porphyrin π-Anion Radicals, and Ni(II) Porphyrin π-Anion Radicals with Some Ni(I) Character

K. M. Kadish,* M. M. Franzen, B. C. Han, C. Araullo-McAdams, and D. Sazou

Contribution from the Department of Chemistry, University of Houson, Houston, Texas 77204-5641. *Received July 2, 1990*

Abstract: The effect of temperature, porphyrin macrocycle, and solvent on the electroreduction of $(P)Ni^{II}$ where P is the dianion of *meso*-tetrakis(*p*-(diethylamino)phenyl)porphyrin ($T(p\text{-}Et_2N)PP$) or *meso*-tetrakis(*o,o,m,m*-tetrafluoro-*p*-(dimethylamino)phenyl)porphyrin ($T(p\text{-}Me_2N)F_4PP$) is reported. Both compounds were reduced by controlled potential electrolysis and characterized by ESR and UV-visible spectroscopy. The site of electron transfer varied as a function of experimental conditions and the stable electrogenerated products were assigned as Ni(I) porphyrins, Ni(II) porphyrin π-anion radicals, or Ni(II) porphyrin π-anion radicals with some Ni(I) character. Ni(I) ESR spectra were obtained for $[(T(p\text{-}Et_2N)PP)Ni]^-$ and $[(T(p\text{-}Me_2N)F_4PP)Ni]^-$ at low temperature in THF under a CO atmosphere as well as in DMF or pyridine under N_2. In contrast, ESR spectra of Ni(II) porphyrin π-anion radicals or Ni(II) porphyrin π-anion radicals with some Ni(I) character were obtained in THF under N_2 at room and low temperature, respectively. $[(T(p\text{-}Et_2N)PP)Ni]^-$ catalytically reduces CH_3I at room temperature, consistent with the presence of some Ni(I) character in the reactive species. $[(T(p\text{-}Me_2N)F_4PP)Ni]^-$ also reacts with CH_3I, but this reaction is not catalytic at room temperature and one or more β pyrrole methylated nickel chlorins are formed as stable products. These species were characterized by UV-visible spectroscopy, ^1H NMR spectroscopy, and mass spectrometry and give data which suggests a high electron density on the porphyrin macrocycle of $[(T(p\text{-}Me_2N)F_4PP)N]^-$.

Introduction

The electroreduction of synthetic nickel(II) porphyrins,[1-9] chlorins[3,6,8] and isobacteriochlorins[6-8] proceeds via one or two one-electron transfer reactions in nonaqueous media. The product of the first reduction may be assigned as a Ni(II) porphyrin π-anion radical, a Ni(I) porphyrin anion, or a mixture of both as shown in Scheme I where L is the dianion of a given porphyrin, chlorin, or isobacteriochlorin ring.

The assignment of Ni(I) in reduced nickel F430[10] and isobacteriochlorins[6-8] is unambiguous, but similar definitive conclusions have not been reached for reduced nickel porphyrins, chlorins, or hydroporphyrins. Initial assignments of reduced nickel porphyrins and chlorins as π-anion radicals were made primarily on the basis of room temperature ESR and UV-visible spectra,[3-5,8] both of which seemed to be definitive. However, more recent results for different Ni(II) porphyrins under different solution conditions indicate that the site of the electroreduction may be all[9] or partially[5,8] at the metal center.

Scheme I

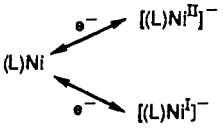

A review of the overall data in the literature seems to suggest that variations in experimental conditions or porphyrin macrocycle can influence the site of electron transfer and/or the electron density on a given singly reduced nickel porphyrin, but little attention has been given to the effect of solvent and the degree of axial ligation. This is discussed in the present paper for two Ni(II) porphyrins which are quite similar in structure, yet have very different half-wave potentials for formation of the singly reduced complex. The structures of these compounds are schematically shown in Figure 1 where ($T(p\text{-}Et_2N)PP$) and ($T(p\text{-}Me_2N)F_4PP$) are the dianions of *meso*-tetrakis(*p*-(diethylamino)phenyl)porphyrin and *meso*-tetrakis(*o,o,m,m*-tetrafluoro-*p*-(dimethylamino)phenyl)porphyrin, respectively.

The two complexes were reduced by controlled potential electrolysis and the resulting products characterized by ESR and thin-layer UV-visible spectroscopy under different solution conditions. Reactions between singly reduced $[(P)Ni]^-$ and CH_3I were also investigated in order to better understand relationships that might exist between thermodynamic potentials, the site of electroreduction, and catalytic reactivity of the reduced complex with alkyl halides.

(1) Kadish, K. M. *Prog. Inorg. Chem.* **1987**, *34*, 435-605.
(2) Kadish, K. M.; Morrison, M. M. *Inorg. Chem.* **1976**, *15*, 980.
(3) Chang, D.; Malinski, T.; Ulman, A.; Kadish, K. M. *Inorg. Chem.* **1984**, *23*, 817.
(4) Kadish, K. M.; Sazou, D.; Liu, Y. M.; Saoiabi, A.; Ferhat, M.; Guilard, R. *Inorg Chem.* **1988**, *27*, 1198.
(5) Kadish, K. M.; Sazou, D.; Maiya, G. B.; Han, B. C.; Liu, Y. M.; Saoiabi, A.; Ferhat, M.; Guilard, R. *Inorg. Chem.* **1989**, *28*, 2542.
(6) Stolzenberg, A. M.; Stershic, M. T. *J. Am. Chem. Soc.* **1988**, *110*, 6391.
(7) Stolzenberg, A. M.; Stershic, M. T. *Inorg. Chem.* **1987**, *26*, 3082.
(8) Renner, M. W.; Forman, A.; Fajer, J.; Simpson, D.; Smith, K. M.; Barkigia, K. M. *Biophys. J.* **1988**, *53*, 277a.
(9) Lexa, D.; Momenteau, M.; Mispelter, J.; Savéant, J.-M.; *Inorg. Chem.* **1989**, *28*, 30.
(10) Jaun, B.; Pfaltz, A. *J. Chem. Soc., Chem. Commun.* **1986**, 1327.

0002-7863/91/1513-512$02.50/0